



PEOPLE'S DEMOCRATIC REPUBLIC OF ALGERIA  
MINISTRY OF HIGHER EDUCATION AND SCIENTIFIC RESEARCH  
IBN KHALDOUN UNIVERSITY – TIARET

# MEMORY

Presented to:

FACULTY OF MATHEMATICS AND COMPUTER SCIENCE  
DEPARTMENT OF COMPUTER SCIENCE

For the attainment of the **Master's** degree

Specialty: software engineering

**For the purpose of creating a startup**

**MindWaveCTRL**

By:



MOUSSELMAL sarra  
BELOUNIS nardjis fatima zohra

On the topic

---

Empowering Brain-Computer Interface (BCI): AI-Based Interpretation of Motor Imagery in EEG Signals.

---

publicly defended on 11 06 2024 in Tiaret to the following jury members:

Mr BEKKI Khadir	MAA	University Ibn-Khaldoun of Tiaret	President
Mrs AMMAR Sabrine	MCB	University Center of Aflou	Supervisor
Mr DAOUD Bachir	MAA	University Ibn-Khaldoun of Tiaret	Co- Supervisor
Mrs LAICHE Fatima	MCB	University Ibn-Khaldoun of Tiaret	Examiner
Mr ANWAR Sekiou	MCB	University Ibn-Khaldoun of Tiaret	Incubator Representative
Mr LABANI Ali		Tiaret Healthcare Institution	Economic Partner Representative

2023-2024

## Acknowledgements

All praise and glory to Almighty (Subhanahu Wa Taalaa) who gave us strength, courage and patience to carry out this work. Peace and blessing of Allah be upon last Prophet Muhammad (Peace Be upon Him).

First of all, I would like to thank Dr DAOUD Bachir and Dr AMMAR Sabrina the directors of this dissertation.

With the greatest words of thanks, gratitude and appreciation for the remarkable and tangible efforts you have made, which have left a clear mark on the success of this work, and we have found nothing but present to you some form of formal letter to express a small part of the extent of our thanks, appreciation and pride. May you have the strength, With our best wishes for progress and success. I would also like to thank all the members of the jury for their interest in our work.

- Dr BEKKI Khadhir
- Dr LAICHE Fatima

Allow us to express our sincere thanks for your effort ,and also big appreciation for your precious time that you spent to evaluate our work, and we thank you very much for directing us to complete our project perfectly.

I would like to extend my thanks to all the members of Techno Foster Incubator and Tiaret University for their contributions to the formation and success of this work. Your support has been invaluable

# Thank you

To my dear parents "**Mousselmal Omar**," my father, and "**Meharzi Saliha**," my mother, for all their efforts in ensuring I received a good education.

To my brothers "**Mouhamed**" and "**Salim**," and my sisters "**Fatiha**" and "**Sihame**," for all their moral support, love, and affection.

To all my friends, especially "**Mouad**," "**idris**," and "**Zakaria**," for their support in the production of this humble work.

Special thanks to the person who inspired this idea, **Nasr-eddine Benkolli**.

To all my colleagues and even my adversaries in Algeria, as well as everyone who has helped me.

*Mpusselmal Sarra*

# Thank you

The journey was neither short nor was the path paved with ease, but I did it. Praise be to **Allah**, who conceals the beginnings and enabled us to reach the ends by His grace and generosity.

I dedicate this success to my **ambitious self** first, which began with ambition and ended with success. Then, to all who supported me in completing my university journey. May you remain a timeless support for me.

To the one for whom Allah made paradise beneath her feet, to the one whose prayers were the secret of my success and whose affection was the balm for my wounds, my role model, my first teacher, and my friend through the days, my dear **mother**. May Allah protect her.

To the one whose name I proudly carry, to the one who strove his whole life for me to be better than him, to the one who supported me without limits and gave me unconditionally, my dear **father**.

To those through whom I grow and upon whom I rely, whose presence gives me strength and boundless love, and with whom I have understood the meaning of life, my sisters and brothers (**Rihab, Hiba, Dhikra, Ali, Idriss**).

Hana and finally the one who said I "got it" for her and I for her, if she wanted against her will, I would not have done it if it had not been for a blessing from God, here is the great day. The day that I was conducted and the hard years of study, I dreamed of it until I was filled with him and his generosity for the joy of completion, thank God that he filled us with good and filled us with pleasure and let me forget my hardship

*Belowis Nardjis*

## Abstract

Brain-Computer Interface (BCI) technology facilitates direct interaction between individuals and computer systems by capturing brain activities, specifically through electroencephalogram (EEG), without relying on physical movement. Our research delves into the realm of 'Motor Imagery,' a BCI modality where users simulate movements mentally, bypassing the need for physical execution. This methodology harnesses brain signals evoked by imagined actions to command external devices. Particularly beneficial for individuals afflicted by conditions like cerebral palsy, stroke, amyotrophic lateral sclerosis, or spinal cord injuries, BCIs aim to restore impaired neural pathways, thereby reinstating lost motor functions. Moreover, leveraging artificial intelligence, notably via Artificial intelligence model enabled data collection, extraction, and signal classification, opens avenues for innovative applications such as 'Thought-Controlled Driving' or 'Mind-Powered Device Operation,' seamlessly translating classification outcomes into actionable commands. Additionally, we believe these technologies can be further enhanced by incorporating the results and performance of the random forest model used in our prototypes, achieving an accuracy of 82.0%, a recall rate of 81.8%, and an F1 score of 81.4%.

**Keywords:** EEG, BCI, artificial intelligence, Motor Imagery, neural rehabilitation

## Résumé

L'interface cerveau-ordinateur (BCI) permet une interaction directe entre les individus et les systèmes informatiques en capturant les activités cérébrales, notamment par électroencéphalogramme (EEG), sans recourir au mouvement physique. Notre recherche explore le domaine de l'« Imagerie Motrice », une modalité BCI où les utilisateurs simulent mentalement des mouvements, contournant ainsi le besoin d'exécution physique. Cette méthodologie exploite les signaux cérébraux évoqués par les actions imaginées pour commander des dispositifs externes. Particulièrement bénéfique pour les personnes atteintes de conditions telles que la paralysie cérébrale, l'accident vasculaire cérébral, la sclérose latérale amyotrophique ou les lésions de la moelle épinière, les BCI visent à restaurer les voies neuronales déficientes, rétablissant ainsi les fonctions motrices perdues. De plus, en tirant parti de l'intelligence artificielle, notamment via la collecte de données, l'extraction et la classification des signaux par Modèle d'intelligence artificielle, de nouvelles applications innovantes telles que la « Conduite par la Pensée » ou l'« Opération de Dispositifs par la Pensée » ouvrent des voies, traduisant sans heurts les résultats de la classification en commandes. De plus, nous croyons que ces technologies peuvent être encore améliorées en incorporant les résultats et les performances du modèle de forêt aléatoire utilisé dans nos prototypes, atteignant une précision de 82,0%, un taux de rappel de 81,8%, et un score F1 de 81,4%.

**Mots clés :** EEG, BCI, intelligence artificielle, Imagerie Motrice, rééducation neuronale.

## ملخص

واجهة الدماغ والحاسوب BCI تسمح بالتفاعل المباشر بين الأفراد والأنظمة الحاسوبية عن طريق التقاط الأنشطة الدماغية، وذلك بواسطة تقنية التخطيط الكهربائي للدماغ (EEG)، دون الحاجة إلى حركة جسدية. تبحث أبحاثنا مجال الصور الحركية، وهي أحد أوضاع (EEG) حيث يقوم المستخدمون بتصوير الحركات عقلياً، متجاوزين بذلك الحاجة للتنفيذ الفعلي. تستغل هذه الطريقة الإشارات الدماغية المحفزة بالأفكار للتحكم في الأجهزة الخارجية. تكون هذه الطريقة مفيدة بشكل خاص للأشخاص الذين يعانون من حالات مثل الشلل الدماغي والسكتة الدماغية والتصلب الجانبي الضموري أو إصابات النخاع الشوكي، حيث تهدف (EEG) إلى استعادة المسارات العصبية المعيبة، وبالتالي استعادة الوظائف الحركية المفقودة. بالإضافة إلى ذلك، عن طريق الاستفادة من الذكاء الاصطناعي، خاصة من خلال جمع البيانات واستخراجها وتصنيفها بواسطة نموذج ذكاء اصطناعي، فإن تطبيقات جديدة مبتكرة مثل القيادة بالتفكير أو التحكم في الأجهزة بالتفكير تفتح آفاقاً جديدة، مترجمة بسلسلة نتائج التصنيف إلى أوامر قابلة للاستخدام. بالإضافة إلى ذلك، نعتقد أنه يمكن تحسين هذه التقنيات بشكل أكبر من خلال دمج نتائج وأداء نموذج الغابة العشوائية المستخدم في نماذجنا الأولية، مما يحقق دقة بنسبة 82%، ومعدل استرجاع بنسبة 81.8%، ونتيجة F1 بنسبة 81.4%.

**الكلمات الرئيسية:** المخطط الكهربائي للدماغ، واجهة الحاسوب والدماغ، الذكاء الاصطناعي، الصور الحركية، إعادة تأهيل عصبي

# Contents

# Contents

<b>Acronym</b>	<b>11</b>
<b>General Introduction</b>	<b>14</b>
Context . . . . .	14
The Problem . . . . .	15
Objective . . . . .	15
Work Plan . . . . .	16
<b>1 General knowledge</b>	<b>18</b>
1.1 Introduction . . . . .	18
1.2 History . . . . .	18
1.3 Frontal Lobe . . . . .	19
1.4 Understanding Motor Imagery . . . . .	20
1.5 Artificial Intelligence . . . . .	21
1.6 Collecting Motor Imagery Data in the Context of Artificial Intelligence . . . . .	21
1.7 Relationship Between Motor Rehabilitation And Collecting Motor Imagery Data In Artificial Intelligence . . . . .	21
1.8 The Concept Of Motor Imaging And Its Neurological Rela- tionships With The Frontal Lobe . . . . .	22
1.9 EEG . . . . .	23
1.9.1 Historic . . . . .	23
1.9.2 Definition . . . . .	24
1.9.3 Types Of electroencephalogram Waves . . . . .	24
1.10 NeuroSky . . . . .	26

1.10.1	Definition . . . . .	26
1.10.2	Device Neurosky ThinkGear AM TGAM EEG . . . . .	26
1.10.3	Components Device . . . . .	27
1.10.4	TGAM Module Features: . . . . .	28
1.10.5	MindViewer . . . . .	28
1.10.6	Brain Signals Handled By A Device . . . . .	29
1.11	Brain-computer interface (BCI) . . . . .	30
1.11.1	Definition . . . . .	30
1.11.2	Fundamental Components Of BCI System . . . . .	30
1.12	Conclusion . . . . .	31
<b>2</b>	<b>Theoretical work</b>	<b>33</b>
2.1	Introduction . . . . .	33
2.2	Mindwave Mobile EEG And Blink Strength Data Acquisition System . . . . .	33
2.3	Data Collection Conditions . . . . .	34
2.4	EEG Signal Preprocessing . . . . .	35
2.4.1	Data Loading And Cleaning . . . . .	35
2.4.2	Deduplication Based On Blink Strength . . . . .	35
2.4.3	Outlier Removal Using IQR Method . . . . .	35
2.4.4	Wavelet-Based Denoising . . . . .	36
2.4.5	Categorizing Eyelash Movements . . . . .	37
2.4.6	Statistical Analysis Of Dataset . . . . .	37
2.5	Conclusion . . . . .	39
<b>3</b>	<b>Classification Algorithms</b>	<b>41</b>
3.1	Introduction . . . . .	41
3.2	K-Nearest Neighbors (KNN): . . . . .	41
3.2.1	Function: . . . . .	41
3.3	Support Vector Machine (SVM): . . . . .	42
3.3.1	Function: . . . . .	42
3.4	Random Forest: . . . . .	43
3.4.1	Function: . . . . .	43

3.4.2	Ensemble Method: . . . . .	43
3.4.3	Bagging: . . . . .	43
3.4.4	Feature Randomness: . . . . .	44
3.5	Correlation Heatmaps . . . . .	44
3.6	Pairwise Scatter Plot . . . . .	44
3.7	SHAP Beeswarm Plot . . . . .	44
3.8	Confusion Matrix . . . . .	45
3.9	Accuracy . . . . .	46
3.10	Recall (Sensitivity) . . . . .	46
3.11	F1 Score . . . . .	46
3.12	Calculate Percentage Of Correct Predictions For Each Model	46
3.13	Calculate Total Correct Predictions Across All Models . . .	47
3.14	Calculate Percentage Of Each Model's Performance Rela- tive To All Models . . . . .	47
3.15	Feature Extraction . . . . .	47
3.15.1	Time-Domain Features . . . . .	48
3.16	Exploratory Data Analysis For Imagery motor Data For Real Motor Data . . . . .	49
3.16.1	Correlation Matrix With Heatmap Before Analyzing And Selecting The Columns . . . . .	49
3.16.2	Pairwise Scatter Plots Before Analyzing And Select- ing The Columns . . . . .	50
3.16.3	Correlation Matrix with Heatmap After analyzing and selecting the columns . . . . .	51
3.16.4	Pairwise Scatter Plots After Analyzing And Select- ing The Columns . . . . .	52
3.17	Exploratory Data Analysis For Imagery Motor And Real Motor Data . . . . .	54
3.17.1	Correlation Matrix With Heatmap Before Analyzing And Selecting The Columns . . . . .	54
3.17.2	Pairwise Scatter Plots Before Analyzing And Select- ing The Columns . . . . .	55

3.17.3	Correlation Matrix With Heatmap After Analyzing And Selecting The Columns First Time . . . . .	56
3.17.4	Pairwise Scatter Plots After Analyzing And Select- ing The Columns First Time . . . . .	57
3.17.5	Correlation Matrix with Heatmap After Analyzing And Selecting The Columns Second Time . . . . .	58
3.17.6	Pairwise Scatter Plots Before Analyzing And Select- ing The Columns Second Time . . . . .	59
3.18	An Example Of The Analytical Method Used To Infer Op- timal Models . . . . .	60
3.18.1	Analysis: Employing The 3 Colomn 'Attention', 'Theta', 'Low Beta' . . . . .	60
3.19	Results of Top Models Across One Datasets . . . . .	64
3.19.1	Results Of Top Model In Dataset of Motor Imagery And Real Motor . . . . .	65
3.20	Conclusion . . . . .	67
<b>4</b>	<b>Implementation And Prototype</b>	<b>69</b>
4.1	Introduction . . . . .	69
4.2	Libraries, Languages, And Tools . . . . .	69
4.2.1	Pandas . . . . .	69
4.2.2	NumPy . . . . .	69
4.2.3	Matplotlib . . . . .	70
4.2.4	Seaborn . . . . .	70
4.2.5	Scikit-learn (sklearn) . . . . .	70
4.2.6	Imbalanced-learn (imblearn) . . . . .	70
4.2.7	Shap . . . . .	70
4.2.8	Pickle . . . . .	70
4.2.9	Anaconda . . . . .	71
4.2.10	Jupyter . . . . .	71
4.2.11	PyNeuro . . . . .	71
4.2.12	Tkinter . . . . .	71
4.2.13	Time . . . . .	71

4.2.14	Pytttsx3 . . . . .	71
4.2.15	Csv . . . . .	72
4.2.16	Python . . . . .	72
4.2.17	NeuroSky's Developer Tools . . . . .	72
4.3	Data Collection Program Design . . . . .	73
4.4	Result of Test In External Data . . . . .	74
4.4.1	Result Of Test In External Data Of Motor Imagery And Real Motor . . . . .	75
4.4.2	Analysis Of Prediction Model Results . . . . .	76
4.4.3	Model Selection Note . . . . .	77
4.5	Real-Time Testing Of The Model . . . . .	78
4.5.1	Brain-Computer Interface (BCI) System Workflow And Applications . . . . .	78
4.5.2	Text Input Application . . . . .	79
4.6	Comparative Study . . . . .	80
4.7	Conclusion . . . . .	82
	<b>General Conclusion And Perspectives</b>	<b>84</b>
	General Conclusion . . . . .	84
	perspectives . . . . .	84

# List of Figures And Table

# List of Figures

1.1	Frontal Lobe Structure[12]. . . . .	20
1.2	Electroencephalogram (EEG)[69]. . . . .	24
1.3	Waveforms Of Different Brain Waves[13]. . . . .	25
1.4	NeuroSky Logo[14]. . . . .	26
1.5	NeuroSky ThinkGear AM TGAM EEG[15]. . . . .	27
1.6	TGAM Module Components[15]. . . . .	28
1.7	MindViewer User Interface[16]. . . . .	29
1.8	The Framework of a Brain-Computer Interface (BCI)[18]. . . . .	30
1.9	Main Components of the Brain-Computer Interface (BCI) System[20]. . . . .	31
2.1	Count of Action: Dataset of Real Motor and Imagery Motor. . . . .	38
2.2	Count Percentage of Action: Dataset of Real Motor and Imagery Motor. . . . .	38
3.1	K-Nearest Neighbors (KNN)[55]. . . . .	42
3.2	Support Vector Machine (SVM)[55]. . . . .	42
3.3	Random Forest[55]. . . . .	43
3.4	EEG Data Processing Pipeline: From Raw Data To Classification. . . . .	47
3.5	Time-Domain Features For Real Motor And Imagery Motor Data 01. . . . .	48
3.6	Time-Domain Features For Real Motor And Imagery Motor Data 02. . . . .	49

3.7	Correlation Matrix With Heatmap Before Analyzing And Selecting The Columns For Real Motor Data. . . . .	50
3.8	Pairwise Scatter Plots Before Analyzing And Aelecting The Columns. . . . .	51
3.9	Correlation Matrix With Heatmap After Analyzing And Se- lecting The Columns For Real Motor Data. . . . .	52
3.10	Pairwise Scatter Plots After Analyzing And Selecting The Columns For Real Motor Data. . . . .	53
3.11	Correlation Matrix With Heatmap Before Analyzing And Selecting The Columns For Imagery Motor And Real Motor Data. . . . .	54
3.12	Pairwise Scatter Plots Before Analyzing And Selecting The Columns For Imagery Motor And Real Motor Data. . . . .	55
3.13	Correlation Matrix With Heatmap After Analyzing And Se- lecting The Columns First Time For Imagery Motor And Real Motor Data. . . . .	56
3.14	Pairwise Scatter Plots After Analyzing And Selecting The Columns First Time For Imagery Motor And Real Motor Data. . . . .	57
3.15	Correlation Matrix With Heatmap After Analyzing And Se- lecting The Columns Second Time For Imagery Motor And Real Motor Data. . . . .	58
3.16	Pairwise Scatter Plots Before Analyzing And Selecting The Columns Second Time For Imagery Motor And Real Motor Data. . . . .	59
3.17	Feature Importances. . . . .	60
3.18	Feature Importance Based On Permutation. . . . .	60
3.19	Model Evaluation. . . . .	61
3.20	Confusion Matrix Of Support Vector Machine. . . . .	62
3.21	Confusion Matrix Of Random Forest Classifier. . . . .	63
3.22	Confusion Matrix Of KNeighbors Classifier. . . . .	64
3.23	Cross-Validation F1 Scores. . . . .	65
3.24	Model Evaluation Metrics. . . . .	66

4.1	Data Collection Console Program . . . . .	74
4.2	Csv File Data . . . . .	74
4.3	Classification Of Real And Imagined Motor Activity Using EEG Signals And Machine Learning In General case[56]. . .	75
4.4	Classification Of Real Motor Blink And Imagined Motor Blink and None Using EEG Signals And Machine Learning[56].	76
4.5	Result Of Test In External Data Of Real Motor Confusion Matrix. . . . .	76
4.6	Brain-Computer Interface (BCI) System Workflow And Applications[57].	79
4.7	Text Input Application. . . . .	79

# List of Tables

4.1	Confusion Matrix For External Data Of Motor Imagery And Real Motor. . . . .	77
-----	---	----

# Acronym

- **AI:** Artificial Intelligence
- **AM:** ASIC Module
- **API:** Application Programming Interface
- **ALS:** Amyotrophic Lateral Sclerosis
- **BCI:** Brain-Computer Interface
- **BMI:** Brain-Machine Interface
- **CT:** Computerized Tomography
- **CSV:** Comma-Separated Values
- **EEG:** electroencephalogram
- **EMI:** Electromagnetic Interference
- **ECoG:** Electrocorticography
- **ESD:** Electrostatic Discharge
- **ERPs:** Event-Related Potentials
- **FN:** False Negatives
- **FP:** False Positives
- **IQR:** Interquartile Range
- **KNN:** K-Nearest Neighbors
- **MRI:** Magnetic Resonance Imaging

- **NET**: Network Enabled Technology
- **PC**: Personal Computer
- **RFC**: Random Forest Classifier
- **SDK**: Software Development Kit
- **SHAP**: SHapley Additive exPlanations
- **SVM**: Support Vector Machine
- **TGAM**: ThinkGear ASIC Module
- **TN**: True Negatives
- **TP**: True Positives

# General Introduction

# General Introduction

## Context

Historically, interest in brain-computer interface (BCI) dates back several decades, with initial studies emerging in the late 20th century. The advancements in radiological and computing technologies during the 1970s facilitated the connection of neural devices to computers, opening new avenues for bridging the gap between the mind and technology. Techniques such as Magnetic Resonance Imaging (MRI) and Computerized Tomography (CT) contributed to a better understanding of brain function and neural activity [1].

In the 1980s and 1990s, emerging technologies saw significant progress, allowing the use of brain imaging techniques to gain more precise insights into brain reactions and activity. Research began to develop methods for recording and analyzing brain activity via computer devices, eventually leading to the emergence of the concept of brain-computer interface as a sophisticated subfield of research [2].

In the past decade, advancements in artificial intelligence and neural signal analysis have led to notable progress in BCI technologies. These technologies have been successfully applied in a wide range of medical and technological applications, making them a central focus for innovation and research in the present time.

## The Problem

Many individuals face debilitating conditions such as cerebral palsy, stroke, amyotrophic lateral sclerosis (ALS), or spinal cord injuries, which severely limit or completely impede their motor functions. Traditional interfaces reliant on physical input fail to accommodate these individuals, exacerbating their sense of dependency and limiting their autonomy.

## Objective

Facing these challenges, our study aims to explore the theoretical foundations, technical implementations, and practical implications of motor imagery-based Brain-Computer Interface (BCI) systems. Through a comprehensive investigation encompassing neuroscience principles, signal processing techniques, and real-world applications, we seek to:

- Investigate the underlying neuronal mechanisms of motor imagery and its relevance for BCI applications;
- Evaluate the effectiveness of signal acquisition methodologies, with a focus on integrating EEG with emerging hardware platforms;
- Explore cutting-edge classification algorithms for decoding EEG signals related to motor imagery;
- Developing and achieving a preliminary model for a BCI system capable of classifying motor imagery in real-time and controlling devices;
- Developing and achieving a preliminary model for a BCI system capable of classifying both motor imagery and actual movement in real-time and controlling devices;
- Developing and achieving a preliminary model for a BCI system capable of classifying both motor imagery and actual movement simultaneously in real-time for studying differences;
- Assess the societal impact, ethical considerations, and future directions of motor imagery-based BCI technology; By addressing these

objectives, we aim to contribute to the continuous advancement and integration of BCI technology into society, fostering innovation, and enhancing the quality of life for individuals with neuromuscular disabilities.

## **Work Plan**

- **Chapter 01:**General knowledge;
- **Chapter 02:**Theoretical work;
- **Chapter 03:**Classification algorithms;
- **Chapter 04:**Implementation And Prototype.

# General knowledge

# Chapter 1

## General knowledge

### 1.1 Introduction

This chapter will delve into EEG-based Brain-Computer Interface (BCI) systems, focusing on NeuroSky's EEG headsets. It covers the fundamental components, such as hardware setup and signal processing algorithms, explaining how EEG signals from the frontal lobe can be used to infer mental intent like motor imagery. The chapter also discusses applications, like controlling external devices through mental commands, and explores future directions to enhance the technology's accuracy and speed.

### 1.2 History

The history of Brain-Computer Interface (BCI) technology dates back to the latter half of the 20th century, where pioneering efforts were made by scientists and researchers in various fields such as neuroscience, electrical engineering, and computer science. In the 1950s and 1960s, initial studies began on recording brain electrical activity using electroencephalography (EEG), laying the groundwork for understanding the basics of recording neural signals.

In 1973, Dutch scientist J. J. R. Rok attempted the first use of motor imagery as a means to interact with external devices. Subsequently,

in the 1980s, the technology began to move towards utilizing motor imagery in BCI applications. In 1988, researchers at the University of Texas developed a system that used motor imagery to control the movement of a wheelchair [1].

Practically, the technology has advanced significantly in the following decades, with increased understanding and advancements in techniques for analyzing and interacting with brain signals. Techniques such as functional magnetic resonance imaging (fMRI) and electrocorticography (ECoG) have become valuable tools in studying and understanding cognitive processes and their applications in BCI.

In recent years, the technology has seen major advancements in the use of artificial intelligence and machine learning to improve the performance of BCI systems, enhancing the accuracy of brain pattern recognition and building more effective predictive models [2]. Thanks to these developments, BCI technology is now capable of offering innovative solutions for device control and enhancing human-computer interaction.

Ongoing studies and research in this field continue to develop and improve BCI technology, with further advancements and innovations expected in the future, expanding its applications and making it more effective and efficient.

### **1.3 Frontal Lobe**

The frontal lobe is the largest lobe in the human brain, located in the anterior part of each cerebral hemisphere. It is known as the brain's command center and plays a crucial role in motor imagery. Notably positioned within the skull, it corresponds to the inner surface of the frontal bone. The frontal lobe is separated from the parietal lobe posteriorly by the central sulcus and from the temporal lobe inferiorly and laterally by the lateral sulcus (Sylvian fissure). On its surface, the frontal lobe contains four major gyri: the precentral gyrus, superior

frontal gyrus, middle frontal gyrus, and inferior frontal gyrus. Its functions encompass several aspects[9], as shown in Figure 1.1:

1. **Prefrontal Cortex:** is manages high-level cognitive functions such as planning, organization, decision-making, and impulse control. Additionally, it significantly influences social behavior and personality expression[8][9].
2. **Motor Cortex:** is responsible for controlling voluntary movements and coordinating body motions. It plays a crucial role in achieving precise and smooth motor execution[8][9].
3. **Broca's Area:** is fundamental in producing the motor aspect of speech. It regulates the necessary muscles for speech production[8][9].

### FRONTAL LOBE SUBSTRUCTURES

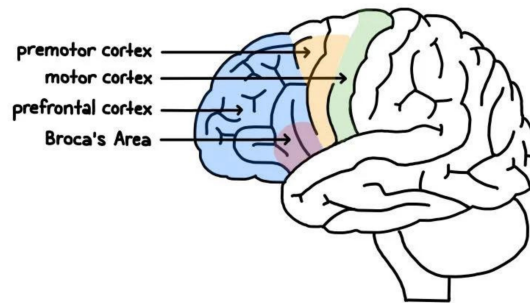


Figure 1.1: Frontal Lobe Structure[12].

## 1.4 Understanding Motor Imagery

Motor imagery is a cognitive process that allows individuals to mentally simulate movements or activities without physically performing them. It involves using imagination and visualization to create vivid mental images of movements in the mind, without the need for actual execution by the body [5].

## 1.5 Artificial Intelligence

Artificial Intelligence (AI) is a field in computer science that deals with creating systems capable of simulating human intelligence and performing tasks that require intelligent thinking. The goal of artificial intelligence is to design and develop systems and software that can use data and experience to make decisions, solve problems, and learn from experiences.

Applications of artificial intelligence span a wide range of fields, including machine learning, big data analysis, natural language processing, robotics, inference systems, video games, healthcare, manufacturing, and many others.

Fundamentally, artificial intelligence relies on a variety of techniques and concepts, including machine learning, artificial neural networks, computational intelligence, inference logic, deep learning, calculus, statistical analysis, and more [6].

## 1.6 Collecting Motor Imagery Data in the Context of Artificial Intelligence

In the realm of artificial intelligence, collecting motor imagery data refers to the process of recording and analyzing neural patterns that occur during the mental simulation of movement, using techniques such as brain imaging with EEG. This type of data aims to understand how the brain interacts with motor imagery and identify the neural patterns associated with it[3].

## 1.7 Relationship Between Motor Rehabilitation And Collecting Motor Imagery Data In Artificial Intelligence

The connection between motor rehabilitation and collecting motor imagery data in artificial intelligence lies in utilizing data collected

from patients during rehabilitation processes to train artificial intelligence models to understand and analyze motor imagery. This data is used to develop artificial intelligence systems capable of identifying and interpreting neural patterns and their interaction with motor imagery[4].

## 1.8 The Concept Of Motor Imaging And Its Neurological Relationships With The Frontal Lobe

Motor imagery is the brain's ability to imagine and perform movements without actually doing them. It's a complex process involving many brain areas, especially the frontal lobe. When we mentally picture moving different body parts, it's like our brain is rehearsing those movements. This "kinetic imagination" activates specific brain networks, which differ depending on which body part we're imagining moving[8].

### 1. Shared Neural Networks:

- **Motor Cortex:** Located in the frontal lobe, it is a major center for motor control. It is divided into subregions, including the primary and secondary motor cortex.
- **Posterior Parietal Cortex:** Located in the parietal lobe and plays an important role in processing sensory information related to the body and movement.
- **Visual Cortex:** Located in the occipital lobe and involved in processing visual information related to movement.
- **Basal Ganglia:** Plays an important role in planning and executing repetitive movements.
- **Cerebellum:** Contributes to the coordination and control of movements.

### 2. The Role Of The Frontal Lobe: The frontal lobe plays a pivotal role in motor perception through:

- **Primary Motor Cortex:** Sends signals to the muscles to control movements.
- **Secondary Motor Cortex:** Involved in the planning and execution of complex movements.
- **Posterior Frontoparietal Region:** Processes sensory information related to the body and movement.
- **Pre-Motor Area:** involved in the planning and execution of successive movements.
- **Working Memory Cortex:** Helps store and retrieve information during motor imagery[8].

## 1.9 EEG

### 1.9.1 Historic

The invention of EEG is generally attributed to the British scientist and physician Richard Caton in 1875. However, it was the German neurologist Hans Berger who, in 1920, first amplified the electrical signal of neuronal activity and described the resulting waveforms. Berger also identified the alpha and beta brain waves. Since then, EEG has evolved, and today we recognize five types of brain waves: delta, theta, alpha, beta, and gamma[1]. In 1932, the British physiologist Edgar Douglas Adrian furthered and completed Berger's work, even earning the Nobel Prize in Physiology. Since the 1950s, EEG has been commonly used in scientific research, including quantitative EEG analysis and electrophysiological brain imaging. While it offers good temporal resolution and is cost-effective, EEG has limitations, such as low spatial resolution and difficulty isolating individual neurocognitive processes. Nevertheless, it remains a valuable tool for detecting neural issues related to various pathologies and measuring brain activity in cognitive neuroscience research[2][3].

### 1.9.2 Definition

EEG is a method used to record the electrical activity of the brain. It involves placing electrodes on the scalp to measure the brain's neuron-generated electrical impulses. These recordings are then utilized to identify brainwave patterns associated with different cognitive states and neurological conditions. EEG is crucial in understanding brain function, as it provides real-time insights into cognitive processes, and neurological disorders. In the realm of Brain-Computer-Interface (BCI), EEG plays a vital role as it serves as the input to decode brain signals, enabling users to interact with computers or external devices using their thoughts. Understanding the basic principles of EEG signal acquisition is fundamental in BCI, as it involves the precise capture and interpretation of these electrical brain signals to translate them into actionable commands, thereby bridging the gap between the brain and technological devices[4]. The shape of the EEG signals is illustrated in Figure 1.2.

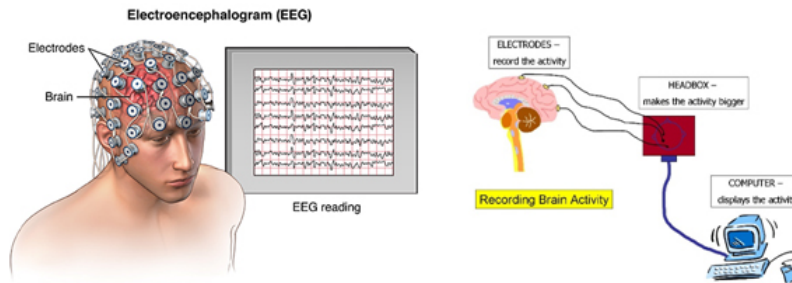


Figure 1.2: Electroencephalogram (EEG)[69].

### 1.9.3 Types Of electroencephalogram Waves

EEG records the spontaneous electrical activity of the brain. Here are the main types of EEG waves. Here are the main types of EEG waves this is illustrated in Figure1.3:

- **Delta Waves** As the slowest of all, these high-amplitude brain

waves have a frequency of 1 to 3 Hz and are experienced by humans when they are asleep.

- **Theta Waves** The Theta waves have a frequency range of 4 to 7 Hz and are found when a person is in a dreamy state. When the waves are close to the lower end, they represent the state when a person hovers between sleep and consciousness. It's also known as the twilight state. Theta waves, in general, signify that mental inefficiency or that the person is either too relaxed or blanked out (zoned out) at that moment.
- **Alpha Waves** The alpha waves have a frequency range of 8 to 12 Hz. These are larger and slower, representing a relaxed or calm state of mind for a person ready to get into action if the need arises. The alpha brain waves are generated when someone feels peaceful after closing their eyes and picturing something they like.
- **Beta Waves** Beta waves are faster and smaller, with a frequency range of 13 to 38 Hz. These waves imply that the person is focused on something. They signify alertness, where the person is in their senses and displays all signs of concentration and mental activity.
- **Gamma Waves** Gamma waves are the fastest ones, with a frequency range of 38 to 42 Hz. These are subtle compared to the other brain waves and work on the consciousness and perception of the person. The waves occur when a person is highly alert and can feel every minute change in their surroundings[5].

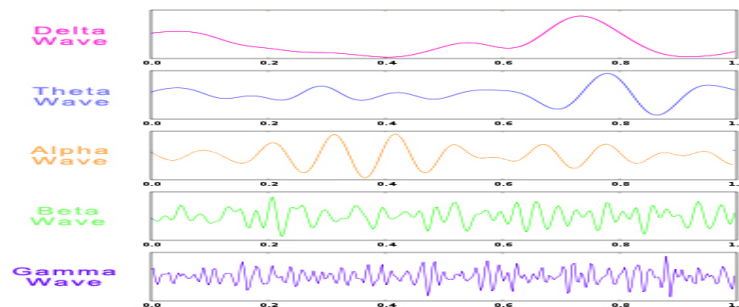


Figure 1.3: Waveforms Of Different Brain Waves[13].

## 1.10 NeuroSky

### 1.10.1 Definition

NeuroSky is a brain-computer interface (BCI) company founded in 2004, focused on developing wearable electroencephalogram (EEG) sensors capable of detecting brainwave activity signals including alpha, beta, theta, delta, and gamma waves. Their flagship consumer products integrate dry-contact EEG electrodes and onboard chipsets to filter, amplify and process these endogenous brain signals into digital data packets readable by computers and mobile devices, commonly via Bluetooth connectivity. Central to their approach is the use of machine learning algorithms to translate recorded EEG rhythms and Event-Related Potentials (ERPs) into proprietary metric outputs claimed to reflect mental states like attention, meditation and eye blinks. The most common product application has been integrating these headset biosensors to enable basic brainwave-driven control in gaming, digital entertainment and wellness training interfaces [6][7], as shown in the NeuroSky logo in Figure 1.4.



Figure 1.4: NeuroSky Logo[14].

### 1.10.2 Device Neurosky ThinkGear AM TGAM EEG

The NeuroSky ThinkGear AM is a biosensor module designed for capturing and processing EEG (Electroencephalogram) signals. It is often used in applications such as brain-computer interfaces (BCI), biofeedback,

and neurofeedback. The ThinkGear technology allows developers to access and utilize EEG data for various purposes, as shown in Figure 1.5.

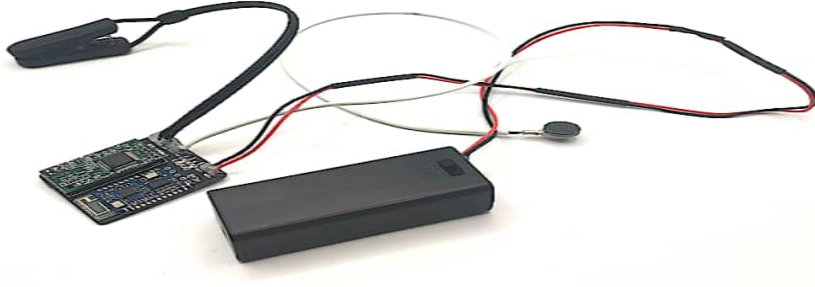


Figure 1.5: NeuroSky ThinkGear AM TGAM EEG[15].

### 1.10.3 Components Device

The components of the NeuroSky ThinkGear AM TGAM EEG device are shown in Figure 1.6 and include:

- **The electrode sheet (Forehead Sensor):** The fabric dry electrode sensor that rests on the forehead to detect electrical signals from the brain[15].
- **Ear Clip Sensor:** The reference sensor clipped to the earlobe used to subtract environmental noise from the forehead sensor signal[15].
- **TGAM Brain Waves Module:** The integrated signal processing chip that analyzes the analog brainwave signal and calculates useful outputs[15].
- **Bluetooth Module:** Enables wireless transmission of data to paired devices and computers up to 10 meters away[15].
- **Battery:** Battery storage holds two cigarette-shaped batteries with a capacity of 1.5 volts each[15].
- **The Shield Line:** This could refer to a shielded cable or a protective shield for the TGAM module, helping to reduce electromagnetic interference (EMI) or noise in the signals[15].

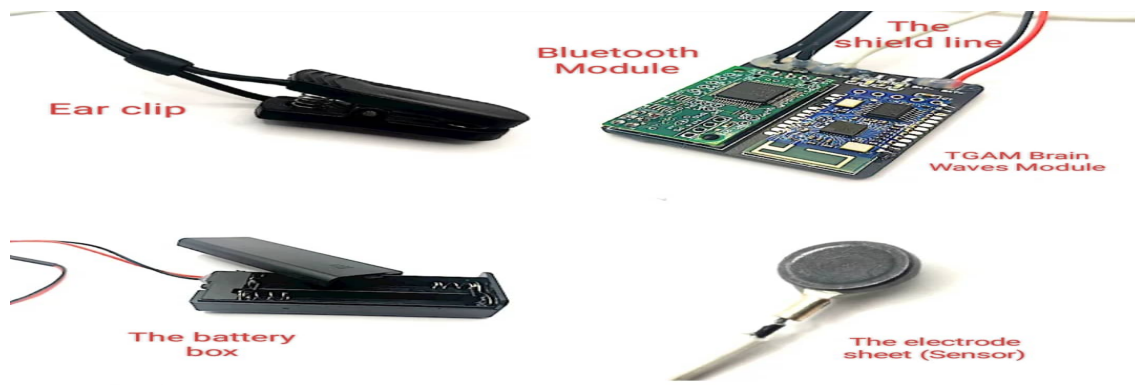


Figure 1.6: TGAM Module Components[15].

#### 1.10.4 TGAM Module Features:

Direct connection to the dry electrode.

One EEG channel + Reference + Ground.

Very weak signal detection capability.

Enhanced high-security filter.

RAW EEGnoiseat 512Hz.

sampling rate:512Hz.

Frequency range: 3-100Hz.

ESD protection. Call To discharge 4kV and 8kV Air.

Maximum consumption: 15mA at 3.3V.

Power supply: 2.97 3.63V.

baud Rate (serial): 1200, 9600, 57600 bits per second. [15][57]

#### 1.10.5 MindViewer

MindViewer is a visualization tool designed for use with the NeuroSky, an EEG device. It allows users to understand their mental states in real-time while engaging in various day-to-day activities such as studying, working, or taking breaks.

When paired with the NeuroSky, MindViewer records and translates brain-wave activity into easily understandable visualizations displayed on a computer or tablet screen, as shown in Figure 1.7. This enables users to monitor their mental state, level of focus, or relaxation while performing their daily tasks.

By utilizing MindViewer, individuals can analyze their own brain activity patterns and understand how different activities impact their minds and performance. This can help them improve their concentration, performance, and overall well-being by optimizing their activities based on real-time feedback from their brain activity.

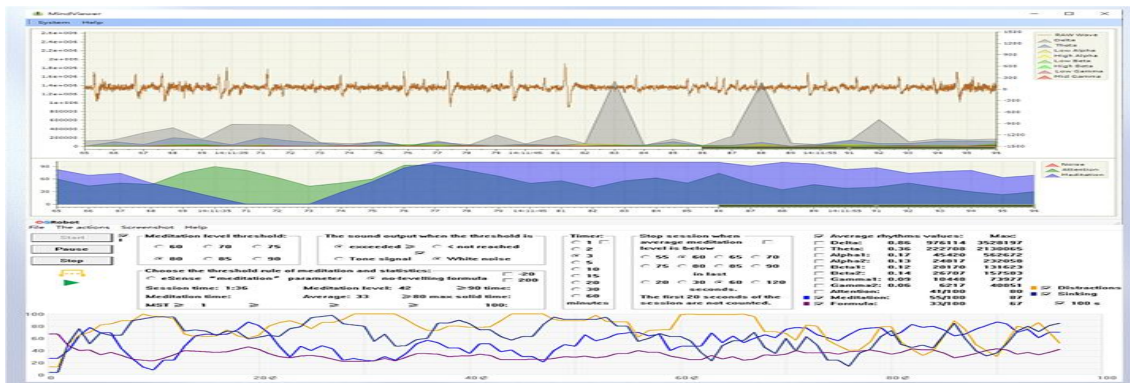


Figure 1.7: MindViewer User Interface[16].

#### 1.10.6 Brain Signals Handled By A Device

- **RAW EEG Signal:** the device provides raw data of brain signals (EEG) at a rate of 512 bits per second.
- **Attention:** the device measures the user's attention level.
- **Meditation:** the device measures the user's meditation level.
- **Eye Blink:** the device can detect blinking.
- **Brain Waves:** the device processes and outputs the EEG frequency spectrum, which includes(Delta, Theta, Alpha, Beta, and Gamma Waves)[17].

## 1.11 Brain-computer interface (BCI)

### 1.11.1 Definition

A brain-computer interface (BCI), also known as a brain-machine interface (BMI), is a system that enables direct communication between the human brain and an external device, bypassing the typical channels of muscles and nerves. It does this by measuring brain activity, such as electrical signals or blood flow changes, and translating those signals into commands that the device can understand, as illustrated in the framework shown in Figure 1.8.

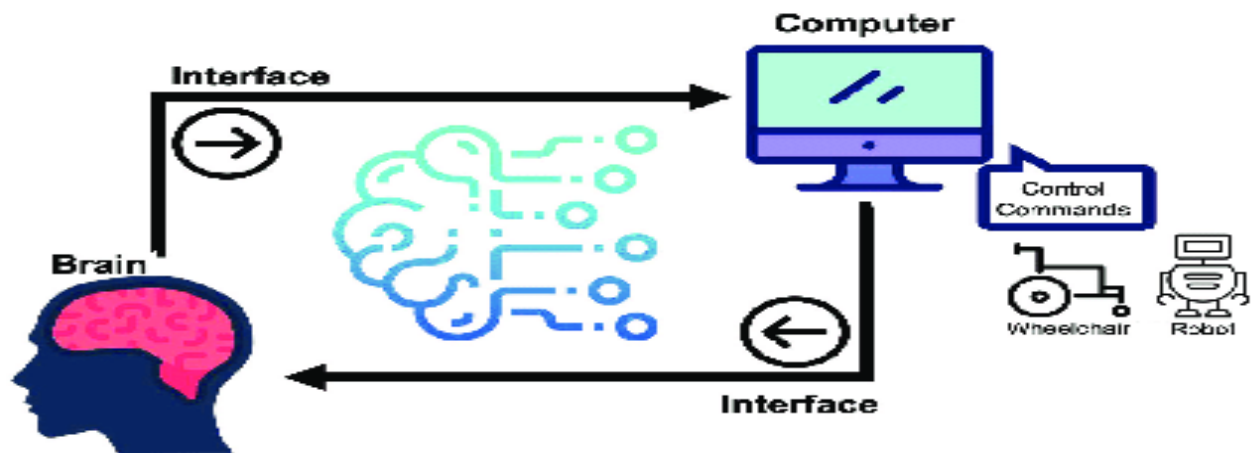


Figure 1.8: The Framework of a Brain-Computer Interface (BCI)[18].

### 1.11.2 Fundamental Components Of BCI System

A typical BCI system comprises three fundamental components, each serving specific roles[19], as shown in Figure 1.9:

1. **Signal Acquisition** This component involves capturing brain signals (such as EEG) from the user's brain. Electrodes or sensors placed on the scalp or directly within the brain record these electrical activities.
2. **Signal Processing** Once acquired, the brain signals undergo processing to extract relevant features. Signal processing techniques enhance the quality of the recorded data and prepare it for interpretation.

- **Feature Extraction** once the signals are acquired, it is necessary to clean them.
- **Feature Classification** once the signals are cleaned, they will be processed and classified to find out which kind of mental task the subject is performing.
- **Feature Translation** once the signals are classified, they will be used by an appropriate algorithm for the development of a certain application.

3. **Application** The processed brain signals are then translated into actionable commands for external devices (e.g., computers, robotic limbs, or virtual environments). BCIs can assist, augment, or restore human cognitive or sensory-motor functions[1].

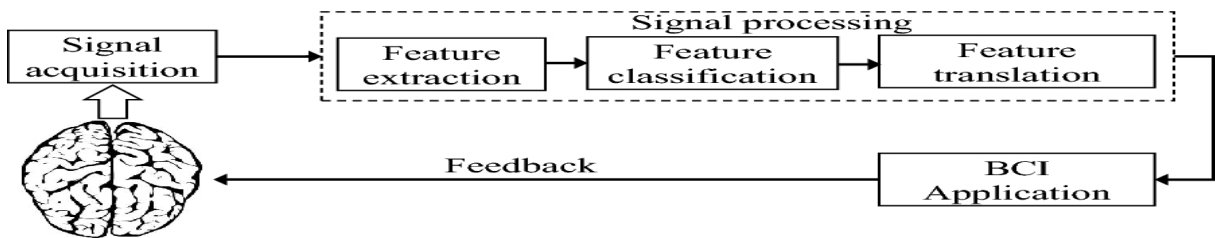


Figure 1.9: Main Components of the Brain-Computer Interface (BCI) System[20].

## 1.12 Conclusion

In this first chapter, we presented brain-computer interfaces (BCIs) and (EEG) to obtain brain signals, decode them, and translate them into executable commands. We learned how to use NeuroSky EEG headsets, in addition to the important role of the frontal lobe in motion control. In the second chapter, let's explore the field of mathematical models and techniques such as filtering and machine learning, which enhances our understanding of EEG signal processing in the context of BCIs.

# Theoretical work

## Chapter 2

# Theoretical work

### 2.1 Introduction

Deciphering motor imagery from (EEG) signals is a critical factor in the development of robust and resilient brain-computer interface (BCI) systems. This chapter explores the theoretical foundations supporting EEG signal processing methodologies, including filtering techniques and artifact removal algorithms. It also delves into the methods used for extracting distinctive features from EEG signals through time-domain, frequency-domain, and time-frequency analyses, which are essential for capturing the unique characteristics of EEG data.

### 2.2 Mindwave Mobile EEG And Blink Strength Data Acquisition System

This Python-based application facilitates real-time acquisition and logging of electroencephalographic (EEG) data and blink strength information from the NeuroSky Mindwave Mobile EEG headset. Using the PyNeuro library, it establishes a Bluetooth connection with the headset, initiates data streaming, and implements callback functions to handle blink events. The application logs timestamped data, including attention, meditation, brainwave frequencies (delta, theta, alpha, beta, gamma), and blink strength values, to a CSV file for a predefined duration. The recorded data can be utilized for further analysis and processing in brain-computer interface

applications. We will discuss this application in more detail in the final chapter, focusing on how it was programmed by our team[23].

### 2.3 Data Collection Conditions

Data was collected from approximately 100 participants using a NeuroSky MindWave headset to record EEG signals. Participants engaged in tasks such as recording blinks and motor imagery while their brain signals were monitored. Strict quality control measures were implemented to ensure data integrity. The collected dataset serves as a valuable resource for exploring brain activity associated with blinking and the cognitive effects of motor imagery in brain-computer interface research. The volunteers were selected from the Mathematics and Computer Science College and Mahdia Hospital, and data collection was conducted following strict procedures and guidelines:

Data was collected in an interference-free environment to avoid distortion from electric fields affecting brainwave frequencies[7].

Volunteers were required to remain fully relaxed with no body movement to minimize stress and anxiety[7].

Participants were selected from diverse age groups to prevent unwanted interference[7].

Data collection duration ranged from 5 to 10 seconds[7].

Rest period: After each attempt, participants receive a short rest period, such as 10 seconds, before proceeding to the next attempt[7].

Volunteers were instructed to blink or imagine blinking regularly[7].

In case of imagining blinking, volunteers signaled with their hand when they felt the need to blink, and recording was immediately stopped and marked with a code "1" to distinguish between imagined and actual blinking[7].

Clear and sudden changes were observed in some brainwaves with direct real-time observation using the naked eye[7].

Recorded files for each person were reviewed immediately after recording to ensure data integrity and absence of interference or anomalies causing data corruption[7].

## 2.4 EEG Signal Preprocessing

Preprocessing of EEG signals is a critical step in the analysis and interpretation of brain activity data. The key stages involved in the EEG signal preprocessing process are as follows:

### 2.4.1 Data Loading And Cleaning

The first stage involves loading the raw EEG data from the data collection process into a structured data format, such as a tabular or matrix representation. Once the data is loaded, various cleaning techniques are applied to ensure the integrity and quality of the dataset. This includes removing duplicate rows, handling missing values, and converting data types to ensure consistent representation of the EEG features[27].

### 2.4.2 Deduplication Based On Blink Strength

In some cases, the collected EEG data may contain duplicate instances, where multiple rows represent the same underlying information, except for the blink strength feature. To address this, a deduplication strategy is employed that identifies sets of duplicate rows based on a subset of the EEG features, excluding the blink strength. From each set of duplicates, the row with the highest blink strength value is retained, ensuring the most informative data point is preserved in the final dataset[28].

### 2.4.3 Outlier Removal Using IQR Method

Outliers in the EEG data can significantly influence the subsequent signal processing and analysis. To mitigate the impact of outliers, a robust technique like the Interquartile Range (IQR) method is implemented. This

approach identifies data points that fall outside a specified range, determined by the first and third quartiles of the data distribution, and removes them from the dataset. Let  $X = \{x_1, x_2, \dots, x_n\}$  be the dataset.

The first quartile (Q1) and third quartile (Q3) are calculated as:

$$Q1 = x_{(\frac{n}{4})}, \quad Q3 = x_{(\frac{3n}{4})} \quad (1)$$

The Interquartile Range (IQR) is calculated as:

$$IQR = Q3 - Q1 \quad (2)$$

The lower bound and upper bound for outlier detection are defined as:

$$\text{Lower bound} = Q1 - k \times IQR, \quad \text{Upper bound} = Q3 + k \times IQR \quad (3)$$

Where  $k$  is a constant threshold, typically set to 1.5. Any data point  $x$  in  $X$  that satisfies  $x < \text{Lower bound}$  or  $x > \text{Upper bound}$  is considered an outlier[22].

#### 2.4.4 Wavelet-Based Denoising

To further enhance the quality of the EEG signals, wavelet-based denoising techniques are applied. This involves performing a discrete wavelet transform on the individual brainwave features, such as Delta, Theta, Alpha, Beta, and Gamma waves. The wavelet coefficients are then subjected to a soft thresholding process to remove high-frequency noise and artifacts, while preserving the underlying signal characteristics.

The wavelet denoising process involves the following mathematical operations:

Let  $f(t)$  be the input signal.

The wavelet decomposition is performed using:

$$W(f) = \{a_j, d_j\} \quad (4)$$

Where  $W(f)$  represents the wavelet transform of the signal  $f(t)$ ,  $a_j$  are the approximation coefficients, and  $d_j$  are the detail coefficients at level  $j$ .

The denoising process involves thresholding the detail coefficients  $d_j$  using a suitable threshold value  $T$  and a thresholding method (soft or hard thresholding):

$$d'_j = \eta(d_j, T) \quad (5)$$

Where  $\eta$  represents the thresholding function, and  $d'_j$  are the thresholded detail coefficients.

The denoised signal  $f'(t)$  is obtained by reconstructing the signal from the approximation coefficients  $a_j$  and the thresholded detail coefficients  $d'_j$  using the inverse wavelet transform:

$$f'(t) = W^{-1}(\{a_j, d'_j\}) \quad (6)$$

The specific mathematical equations for the wavelet transform and its inverse are defined by the chosen wavelet basis function and are handled by the PyWavelets library functions (`pywt.wavedec`, `pywt.threshold`, and `pywt.waverec`)[25].

#### 2.4.5 Categorizing Eyelash Movements

The EEG signal preprocessing workflow includes the addition of a new 'Action' column to the dataset, which categorizes eyelash movements based on blink strength. A threshold is defined to differentiate intentional eye blinks/winks from natural occurrences. The 'Action' column is then populated, with a value of 1 indicating an intentional eye blink, and 0 representing the baseline or resting state[24][23].

#### 2.4.6 Statistical Analysis Of Dataset

##### Dataset Of Real Motor And Imagery Motor

The dataset explores how people engage with real and imagined movements through eye blink, offering insights into the parallels and distinctions between actual and imagined performance, as shown in Figures 2.1 and 2.2.

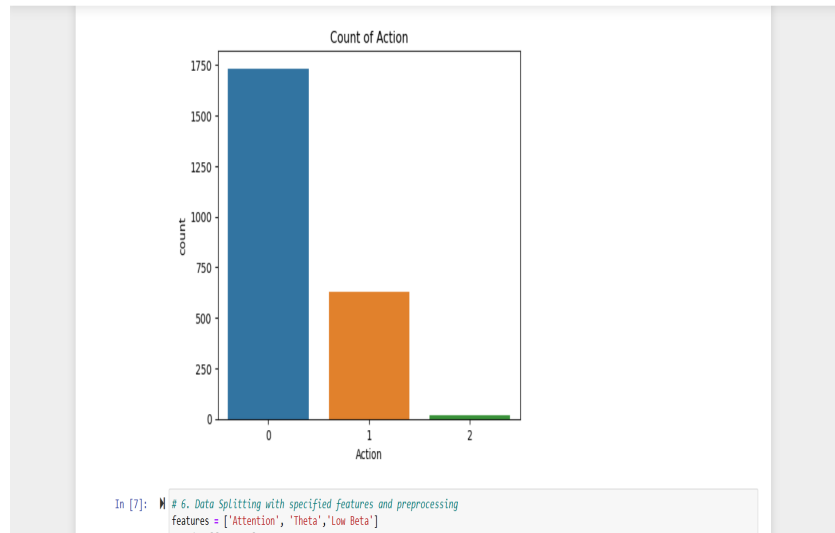


Figure 2.1: Count of Action: Dataset of Real Motor and Imagery Motor.

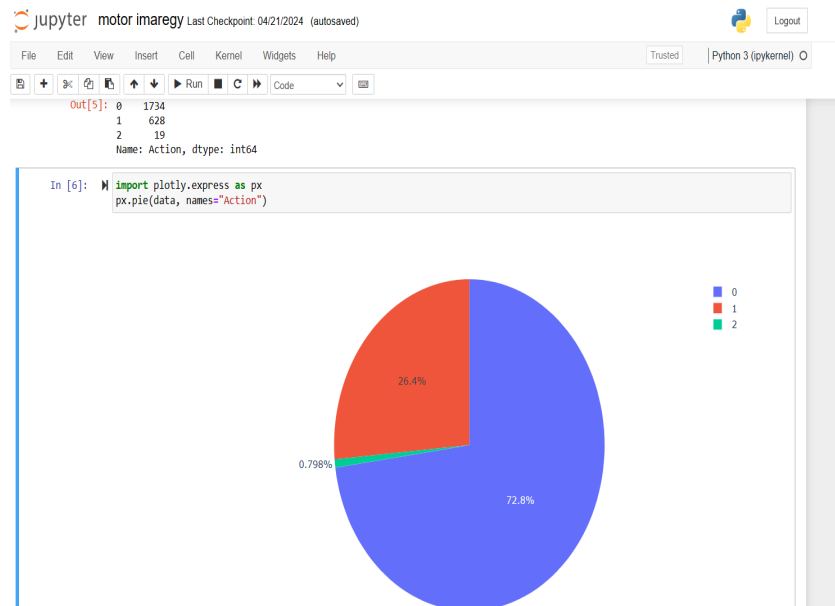


Figure 2.2: Count Percentage of Action: Dataset of Real Motor and Imagery Motor.

## 2.5 Conclusion

Casting the chapter's conclusion, it underscores the significance of decoding motor imagery from EEG signals in developing robust and resilient BCI systems. We've delved into the theoretical foundations of EEG signal processing, encompassing filtering techniques and artifact removal algorithms. This theoretical inquiry reveals challenges to overcome for enhancing the accuracy and efficiency of BCI systems. In the forthcoming chapter, we'll delve into feature selection and classification algorithms to effectively and accurately analyze and classify EEG signals, thereby bolstering BCI system capabilities and paving the way for novel and exciting applications in the future.

# Classification Algorithms

## Chapter 3

# Classification Algorithms

### 3.1 Introduction

In this chapter, we will focus on classification and analysis algorithms to identify the most impactful features and algorithms that significantly affect the data results. We will delve into real motor data, imagery motor data, and real motor and imagery motor data separately, presenting the analysis stages leading to the desired outcomes.

### 3.2 K-Nearest Neighbors (KNN):

KNN predicts by averaging the outcomes of the nearest neighbor samples. It's a simple, effective method for classification and regression[31], as illustrated in Figure 3.1.

#### 3.2.1 Function:

$$\hat{y} = \frac{1}{k} \sum_{i=1}^k y_i \quad (7)$$

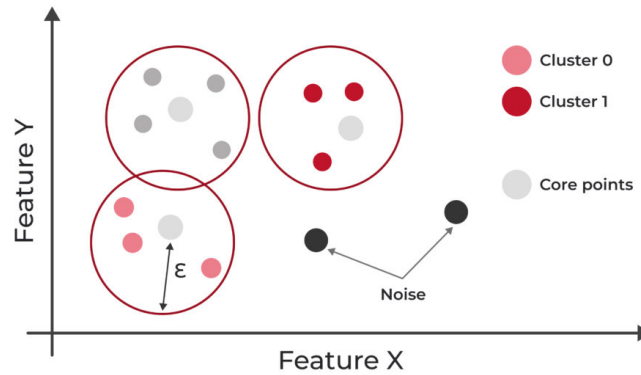


Figure 3.1: K-Nearest Neighbors (KNN)[55].

### 3.3 Support Vector Machine (SVM):

SVM seeks the best margin between classes using support vectors and hyperplanes, suitable for both linear and non-linear problems[28], as shown in Figure 3.2.

#### 3.3.1 Function:

$$f(x) = w \cdot x + b \tag{8}$$

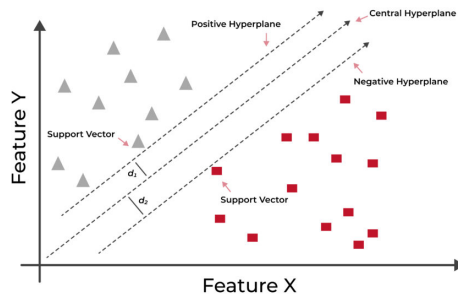


Figure 3.2: Support Vector Machine (SVM)[55].

### 3.4 Random Forest:

Random Forest builds multiple decision trees and merges them to get a more accurate and stable prediction. It's great for classification and regression, reducing overfitting and handling large datasets with high dimensionality[29], as illustrated in Figure 3.3.

#### 3.4.1 Function:

$$\hat{y} = \frac{1}{n} \sum_{i=1}^n \text{tree}_i(x) \quad (9)$$

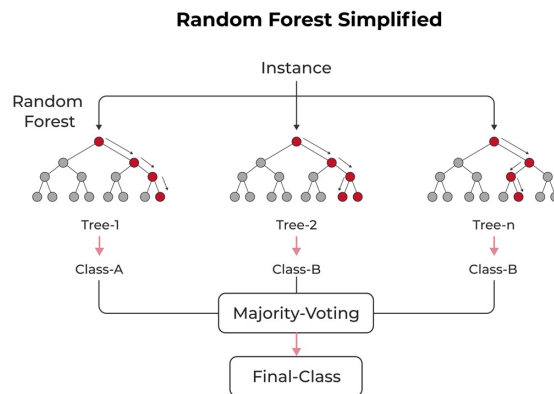


Figure 3.3: Random Forest[55].

#### 3.4.2 Ensemble Method:

It combines the predictions from multiple trees to improve accuracy.

#### 3.4.3 Bagging:

Each tree is trained on a random subset of the data, increasing diversity and robustness.

#### 3.4.4 Feature Randomness:

Randomly selects a subset of features for splitting nodes, which contributes to variance reduction.

### 3.5 Correlation Heatmaps

Correlation heatmaps visualize the strength of relationships between numerical variables. Each variable is represented by a column and each pairwise relationship by a row. The cell values indicate the strength and direction of the relationship, with positive values for positive relationships and negative values for negative relationships. The color-coding of the cells allows for quick identification of these relationships. Correlation heatmaps help identify potential relationships, outliers, and both linear and nonlinear relationships between variables[32].

### 3.6 Pairwise Scatter Plot

A pairwise scatter plot, also known as a scatter plot matrix, is a grid of scatter plots that shows the relationships between pairs of variables in a dataset. Each cell in the grid represents a scatter plot of one variable against another. This type of plot is useful for visualizing the pairwise relationships and potential correlations among multiple variables simultaneously[33].

### 3.7 SHAP Beeswarm Plot

The SHAP beeswarm plot visualizes the distribution of SHAP values across features in a dataset. Resembling a swarm of bees, the arrangement of points reveals insights into the role and impact of each feature on the model's predictions. On the plot's x-axis, dots represent the SHAP values of individual data instances, providing crucial information about feature influence. A wider spread or higher density of dots indicates more significant variability or a more substantial impact on the model's predictions.

This allows us to evaluate the significance of features in contributing to the model's output.

Additionally, the plot employs a default color mapping on the y-axis to represent low or high values of the respective features. This color scheme aids in identifying patterns and trends in the distribution of feature values across instances[34].

### 3.8 Confusion Matrix

A confusion matrix is a matrix that summarizes the performance of a machine learning model on a set of test data. It is a means of displaying the number of accurate and inaccurate instances based on the model's predictions. It is often used to measure the performance of classification models, which aim to predict a categorical label for each input instance.

The matrix displays the number of instances produced by the model on the test data.[35]:

- True positives (TP): occur when the model accurately predicts a positive data point;
- True negatives (TN): occur when the model accurately predicts a negative data point;
- False positives (FP): occur when the model predicts a positive data point incorrectly;
- False negatives (FN): occur when the model mispredicts a negative data point

### 3.9 Accuracy

Accuracy is the ratio of the number of correct predictions to the total number of predictions.

$$\begin{aligned}\text{Accuracy} &= \frac{\text{Number of correct predictions}}{\text{Total number of predictions}} \\ &= \frac{TP + TN}{TP + TN + FP + FN}\end{aligned}\tag{11}$$

### 3.10 Recall (Sensitivity)

Recall, also known as sensitivity, is the ratio of true positives to the sum of true positives and false negatives.

$$\text{Recall} = \frac{TP}{TP + FN}\tag{12}$$

### 3.11 F1 Score

The F1 Score is the harmonic mean of precision and recall.

$$\text{F1 Score} = 2 \times \frac{\text{Precision} \times \text{Recall}}{\text{Precision} + \text{Recall}} = \frac{2 \times TP}{2 \times TP + FP + FN}\tag{13}$$

### 3.12 Calculate Percentage Of Correct Predictions For Each Model

$$\text{Percentage of correct predictions} = \text{Accuracy} \times 100\tag{14}$$

### 3.13 Calculate Total Correct Predictions Across All Models

$$\text{Total correct predictions} = \sum_{i=1}^n \text{Accuracy}_i \times \text{Total} \quad (15)$$

- **Total** represents the total number of predictions made across all models.
- **n** represents the number of models.

### 3.14 Calculate Percentage Of Each Model's Performance Relative To All Models

$$\text{RPP}_i = \frac{\text{Accuracy}_i \times \text{Total}}{\text{Total correct predictions across all models}} \times 100 \quad (16)$$

### 3.15 Feature Extraction

Feature extraction is a crucial step in the analysis of EEG data, as it involves the identification and quantification of relevant characteristics from the raw signals. These features serve as inputs to the subsequent machine learning and classification models, enabling the interpretation of cognitive states and the development of brain-computer interface (BCI) applications. This process is illustrated in Figure 3.4.

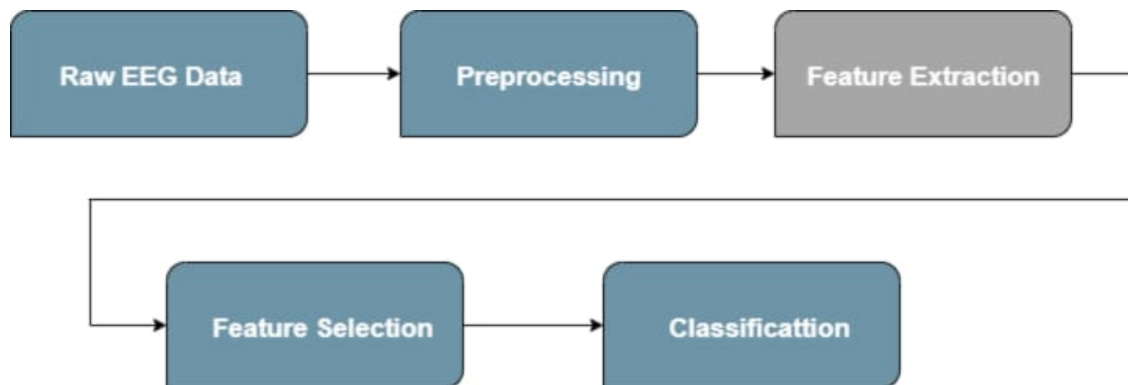


Figure 3.4: EEG Data Processing Pipeline: From Raw Data To Classification.

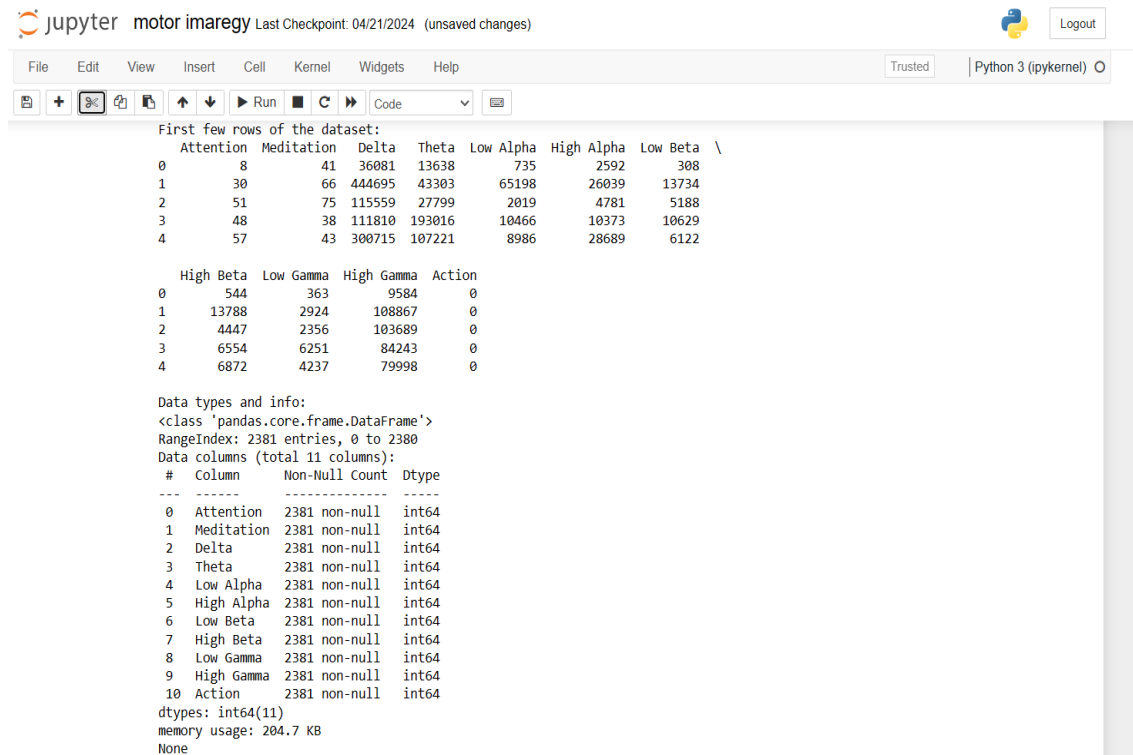
### 3.15.1 Time-Domain Features

Time-domain analysis provides valuable insights into the temporal dynamics of EEG signals. In this study, we comprehensively analyzed time-domain features for each data[36]

## Time-Domain Features For Imagery Motor And Real motor Data

The dataset contains 2381 rows of integer values reflecting brainwave activities and actions, mostly binary with a mean of 0.279714. Key measures include mean attention (51.29) and meditation (54.60), with wide-ranging frequencies like delta (mean: 469,053) and theta (mean: 113,832).

As shown in Figure 3.5 and Figure 3.6, the dataset contains time-domain features for imagery motor and real motor data.



The screenshot shows a Jupyter Notebook interface with the following content:

```

jupyter motor imaregy Last Checkpoint: 04/21/2024 (unsaved changes)
File Edit View Insert Cell Kernel Widgets Help Trusted Python 3 (ipykernel)
First few rows of the dataset:
   Attention  Meditation  Delta  Theta  Low Alpha  High Alpha  Low Beta  \
0          8          41  36081  13638          735          2592          308
1         30          66  444695  43303         65198         26039         13734
2         51          75  115559  27799          2019          4781          5188
3         48          38  111810  193016         10466         10373         10629
4         57          43   300715  107221          8986         28689          6122

   High Beta  Low Gamma  High Gamma  Action
0          544          363          9584          0
1        13788         2924         108867          0
2        44447         2356         103689          0
3        6554         6251          84243          0
4        6872         4237          79998          0

Data types and info:
<<class 'pandas.core.frame.DataFrame'>
RangeIndex: 2381 entries, 0 to 2380
Data columns (total 11 columns):
#  Column  Non-Null Count  Dtype
---  ---  ---
0  Attention  2381 non-null    int64
1  Meditation  2381 non-null    int64
2  Delta      2381 non-null    int64
3  Theta     2381 non-null    int64
4  Low Alpha  2381 non-null    int64
5  High Alpha 2381 non-null    int64
6  Low Beta   2381 non-null    int64
7  High Beta  2381 non-null    int64
8  Low Gamma  2381 non-null    int64
9  High Gamma 2381 non-null    int64
10 Action    2381 non-null    int64
dtypes: int64(11)
memory usage: 204.7 KB
None

```

Figure 3.5: Time-Domain Features For Real Motor And Imagery Motor Data 01.

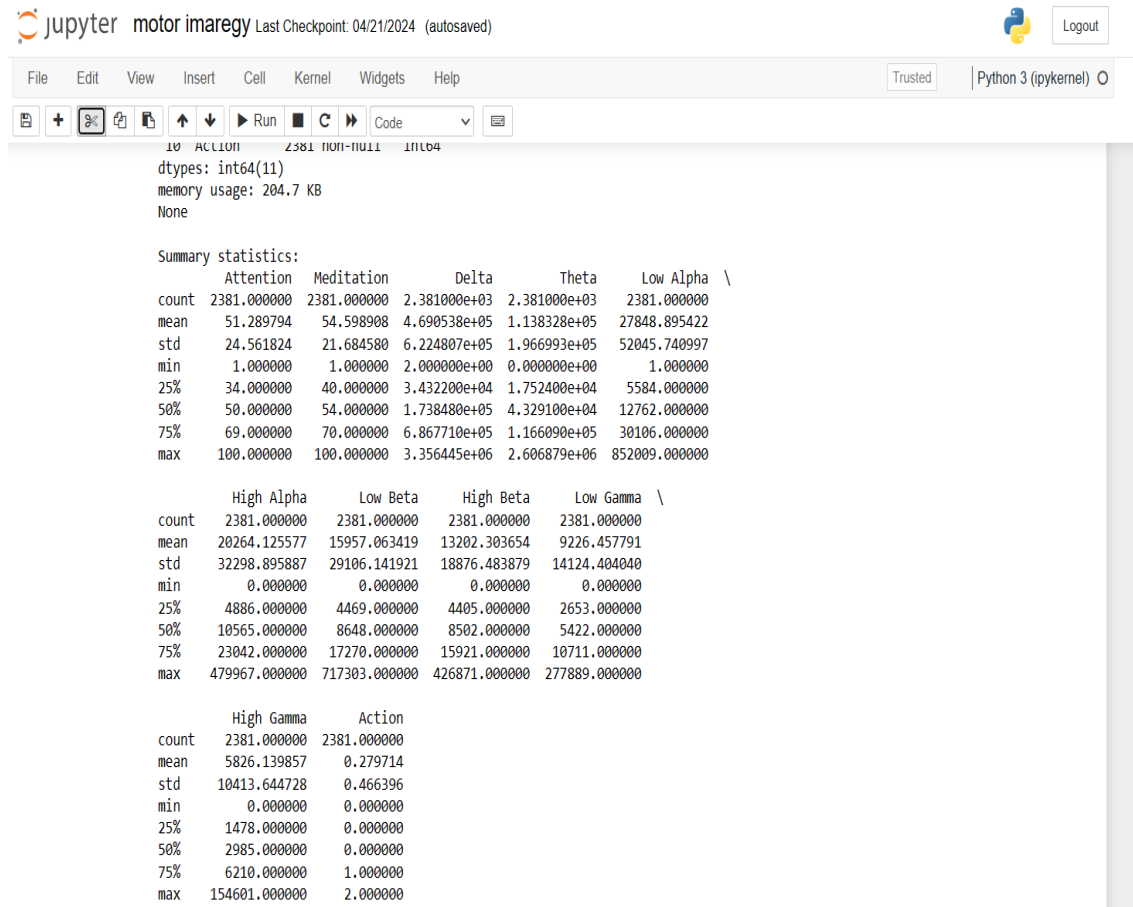


Figure 3.6: Time-Domain Features For Real Motor And Imagery Motor Data 02.

## 3.16 Exploratory Data Analysis For Imagery motor Data For Real Motor Data

### 3.16.1 Correlation Matrix With Heatmap Before Analyzing And Selecting The Columns

The most influential relationships with the target variable 'Action' for predicting eye movement are 'High Gamma' ( $r=0.055$ ), 'Low Gamma' ( $r=0.053$ ), and 'Attention' ( $r=0.05$ ). These correlations indicate their importance in eye movement prediction, providing valuable insights for scientific analysis. As shown in Figure 3.11.

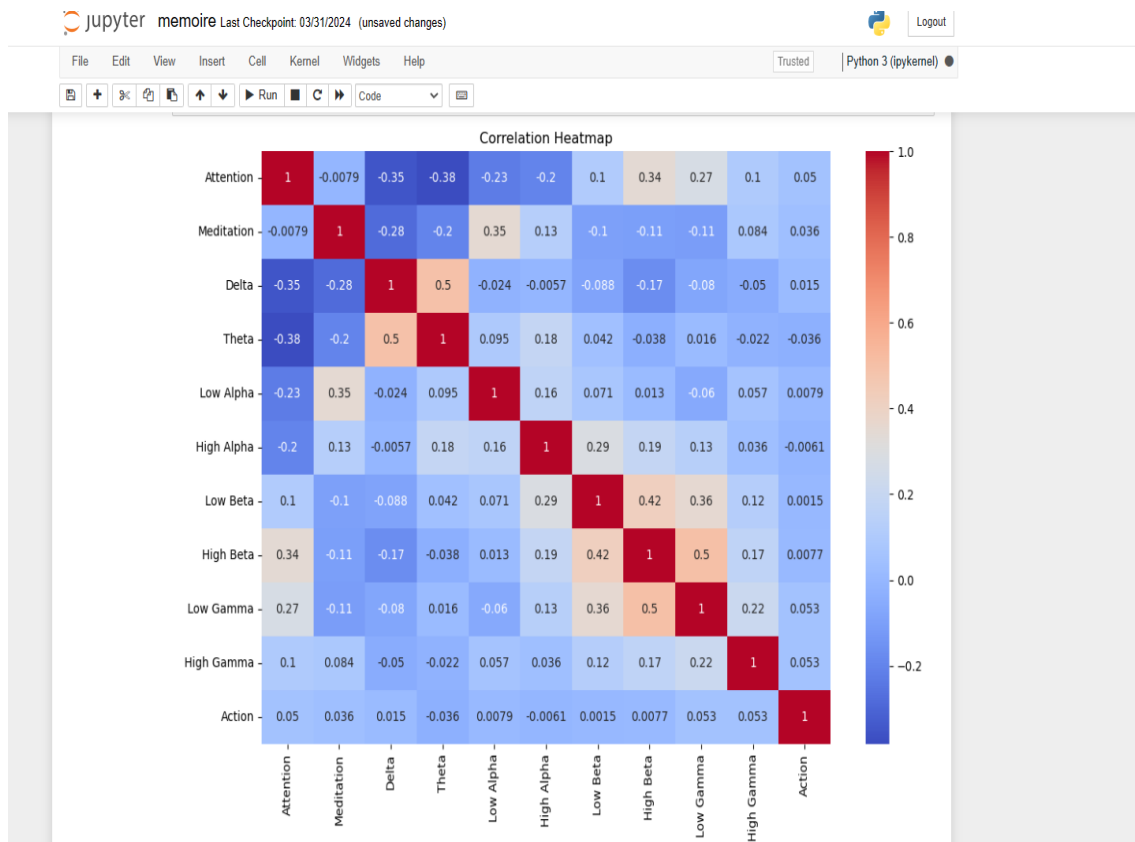


Figure 3.7: Correlation Matrix With Heatmap Before Analyzing And Selecting The Columns For Real Motor Data.

### 3.16.2 Pairwise Scatter Plots Before Analyzing And Selecting The Columns

The pairwise scatter plots reveal that Theta and Attention exhibit the strongest associations with the target variable Action, showing distinct clustering and separation of Action categories. Low Beta and Low Alpha provide complementary predictive power when combined with Theta, while High Beta, Meditation, High Gamma, High Alpha, Low Gamma, and Delta appear to be weaker features with limited discriminative ability for this motor imagery dataset. As shown in Figure 3.12.

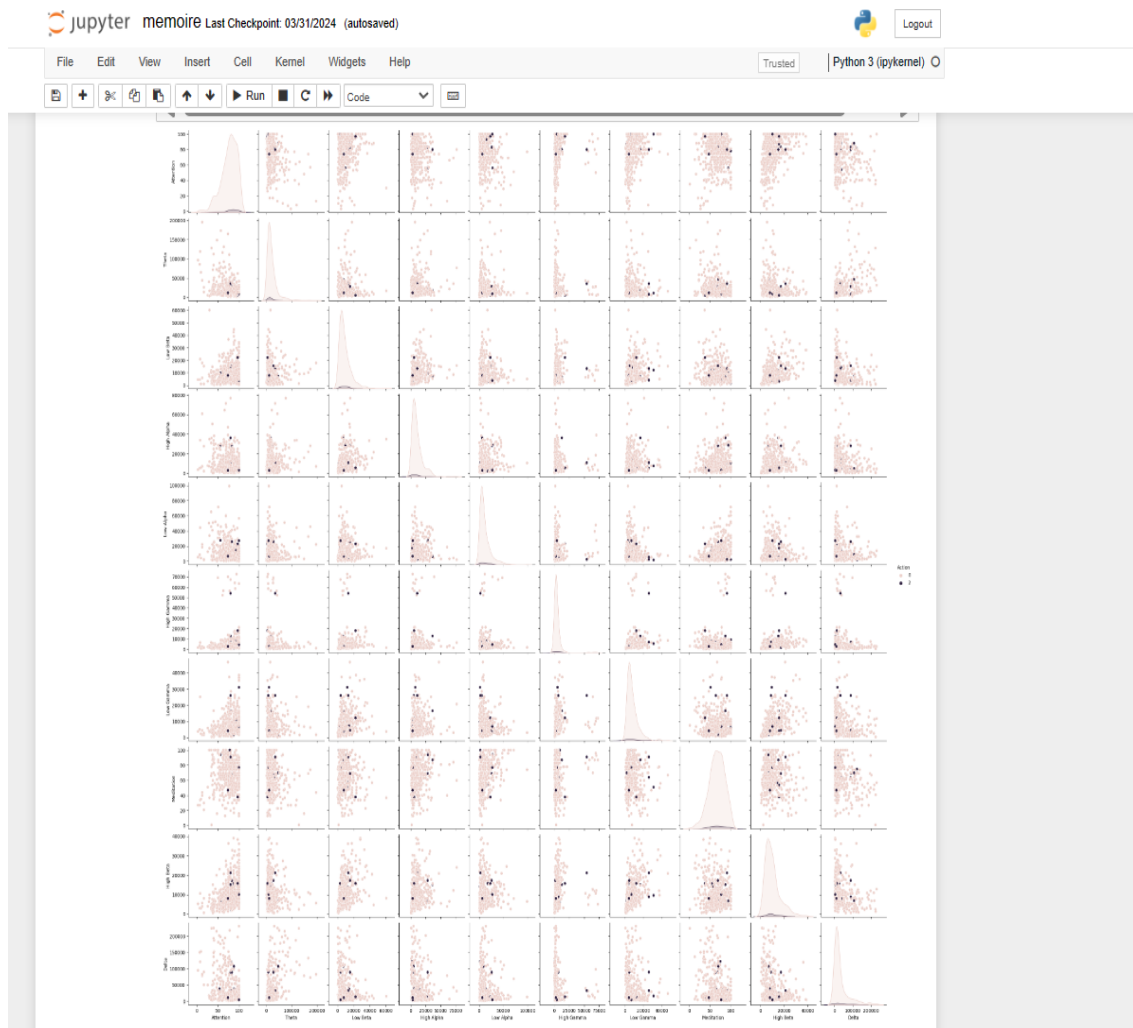


Figure 3.8: Pairwise Scatter Plots Before Analyzing And Aeselecting The Columns.

### 3.16.3 Correlation Matrix with Heatmap After analyzing and selecting the columns

The heat map analysis reveals the most influential relationships with the target variable 'Action': **Attention** ( $r = 0.05$ ) shows a weak positive correlation, suggesting a slight association with eye movement; **Theta** ( $r = -0.036$ ) displays a weak negative correlation, indicating a minor inhibitory relationship; and **Low Beta** ( $r = 0.0015$ ) has a negligible positive correlation, implying minimal influence on the target variable. As shown in Figure 3.9.

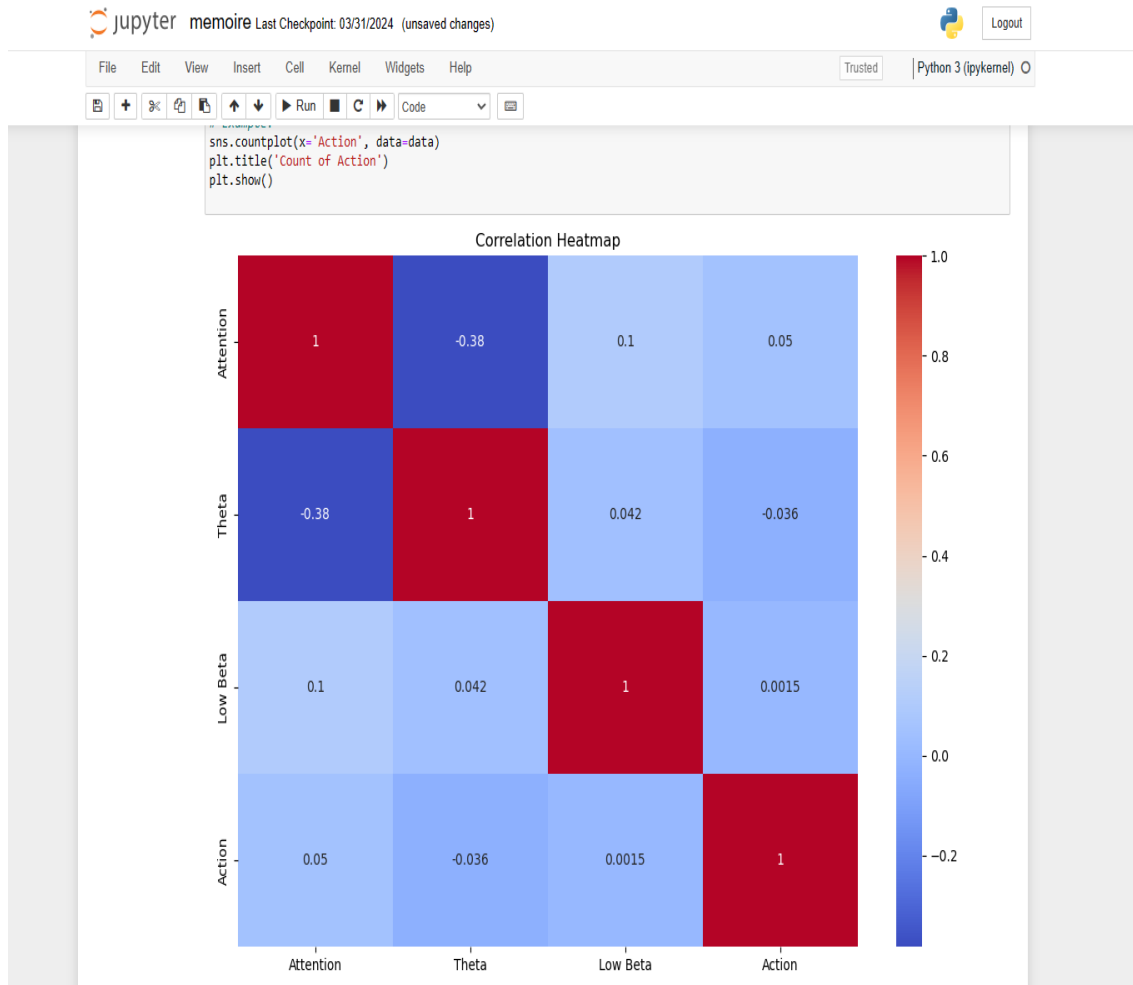


Figure 3.9: Correlation Matrix With Heatmap After Analyzing And Selecting The Columns For Real Motor Data.

#### 3.16.4 Pairwise Scatter Plots After Analyzing And Selecting The Columns

The chart shows distributions and scatter plots for “Attention,” “Theta,” and “Low Beta,” colored by the binary “Action” variable (0 or 2). “Low beta” displays the most pronounced separation between the “Action” categories, suggesting that it is a strong predictor, while “Attention” also shows a significant association. As shown in Figure 3.10.

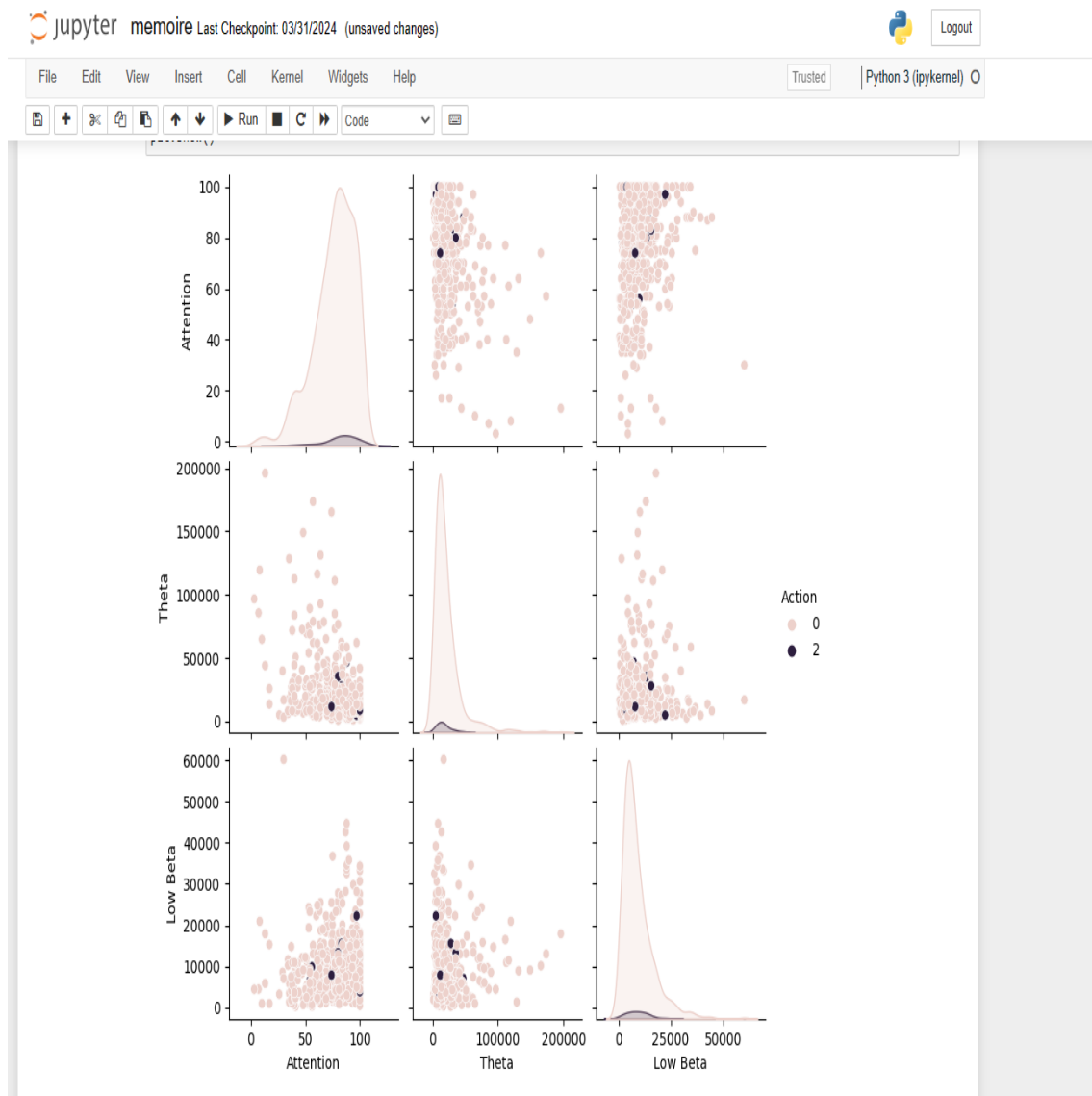


Figure 3.10: Pairwise Scatter Plots After Analyzing And Selecting The Columns For Real Motor Data.

## 3.17 Exploratory Data Analysis For Imagery Motor And Real Motor Data

### 3.17.1 Correlation Matrix With Heatmap Before Analyzing And Selecting The Columns

The most influential relationships with the target variable "Action" are as follows: **Attention** has the strongest negative correlation ( $r = -0.17$ ), indicating that higher attention levels may reduce task performance. **Meditation** also negatively correlates ( $r = -0.14$ ), suggesting that higher meditation states lower cognitive engagement. **Theta** ( $r = 0.12$ ) enhances task performance, while **Low Beta** ( $r = 0.069$ ), **Low Gamma** ( $r = 0.042$ ), and **High Gamma** ( $r = 0.03$ ) show positive correlations. As shown in Figure 3.11.

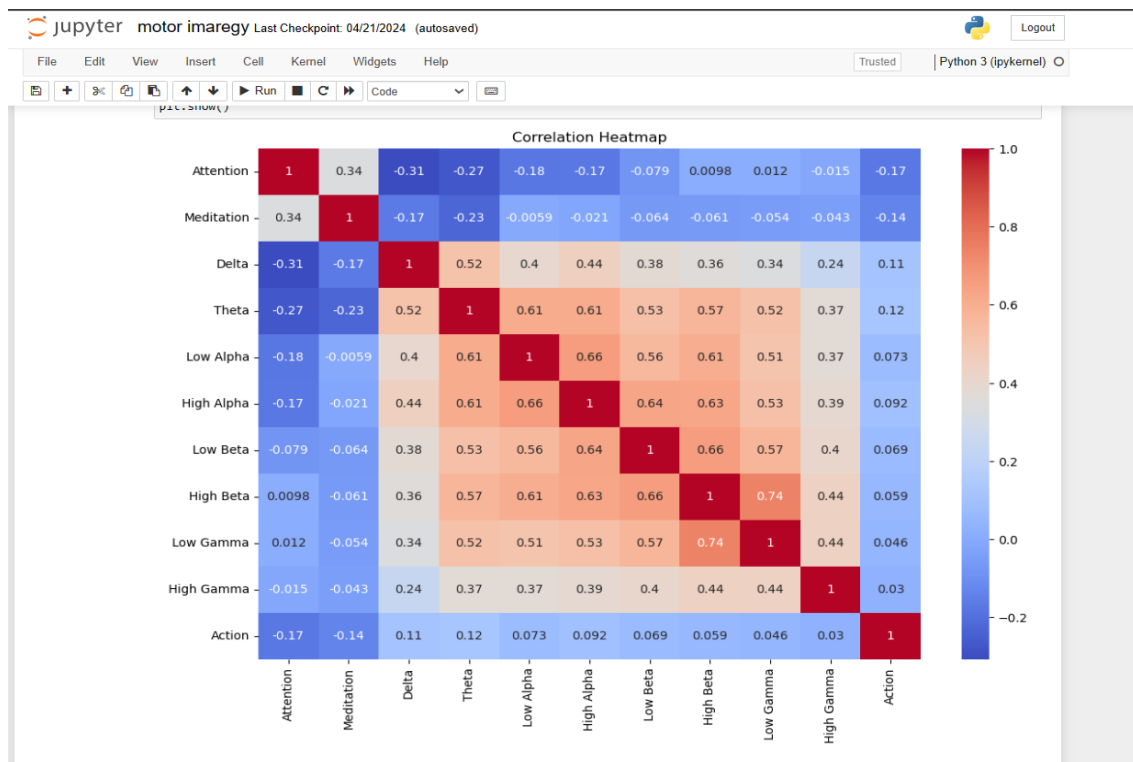


Figure 3.11: Correlation Matrix With Heatmap Before Analyzing And Selecting The Columns For Imagery Motor And Real Motor Data.

### 3.17.2 Pairwise Scatter Plots Before Analyzing And Selecting The Columns

The pairwise scatter plots reveal that Theta and Attention are the strongest predictors of the three Action categories (0, 1, 2), exhibiting distinct clustering and separation. Low Beta and Low Alpha provide complementary information, while High Beta, Meditation, High Gamma, High Alpha, Low Gamma, and Delta appear to be weaker features with limited discriminative power for this motor imagery dataset. As shown in Figure 3.12.

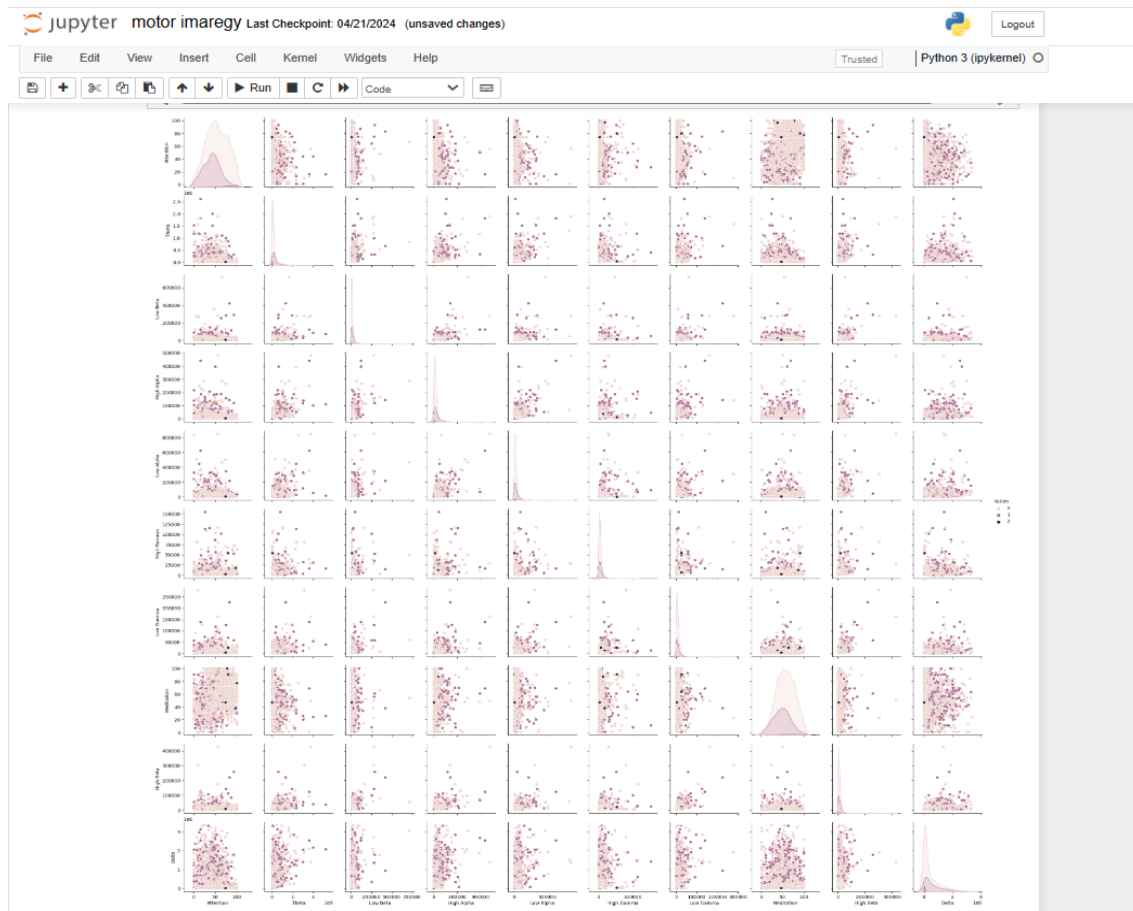


Figure 3.12: Pairwise Scatter Plots Before Analyzing And Selecting The Columns For Imagery Motor And Real Motor Data.

### 3.17.3 Correlation Matrix With Heatmap After Analyzing And Selecting The Columns First Time

Heat map analysis reveals the most influential relationships with the target variable “Action”: “Attention” ( $r=-0.17$ ), “Low Beta” ( $r=0.069$ ), and “Theta” ( $r=0.12$ ). These variables show the strongest correlations, with “attention” showing a significant negative relationship, and “theta” and “low beta” showing significant positive correlations, indicating their significant influence on the target variable. As depicted in Figure 3.13.

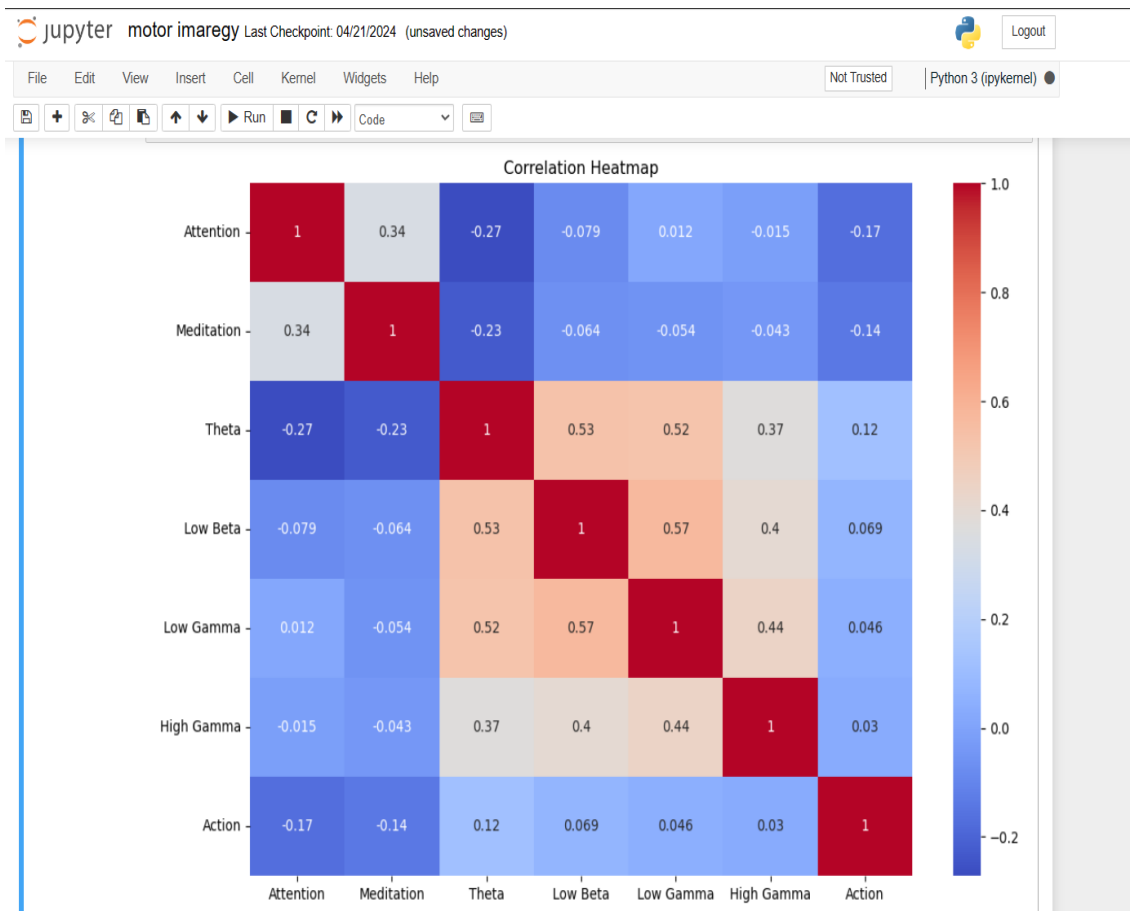


Figure 3.13: Correlation Matrix With Heatmap After Analyzing And Selecting The Columns First Time For Imagery Motor And Real Motor Data.

### 3.17.4 Pairwise Scatter Plots After Analyzing And Selecting The Columns First Time

The pairwise scatter plots reveal that 'Theta' and 'Attention' are the strongest predictors of the target variable 'Action', with 'Low Beta' providing additional discriminative power when combined with the other features. 'High Beta' appears to be the weakest predictor but may still contribute to the overall model performance when used in conjunction with the more informative features. As shown in Figure 3.14.

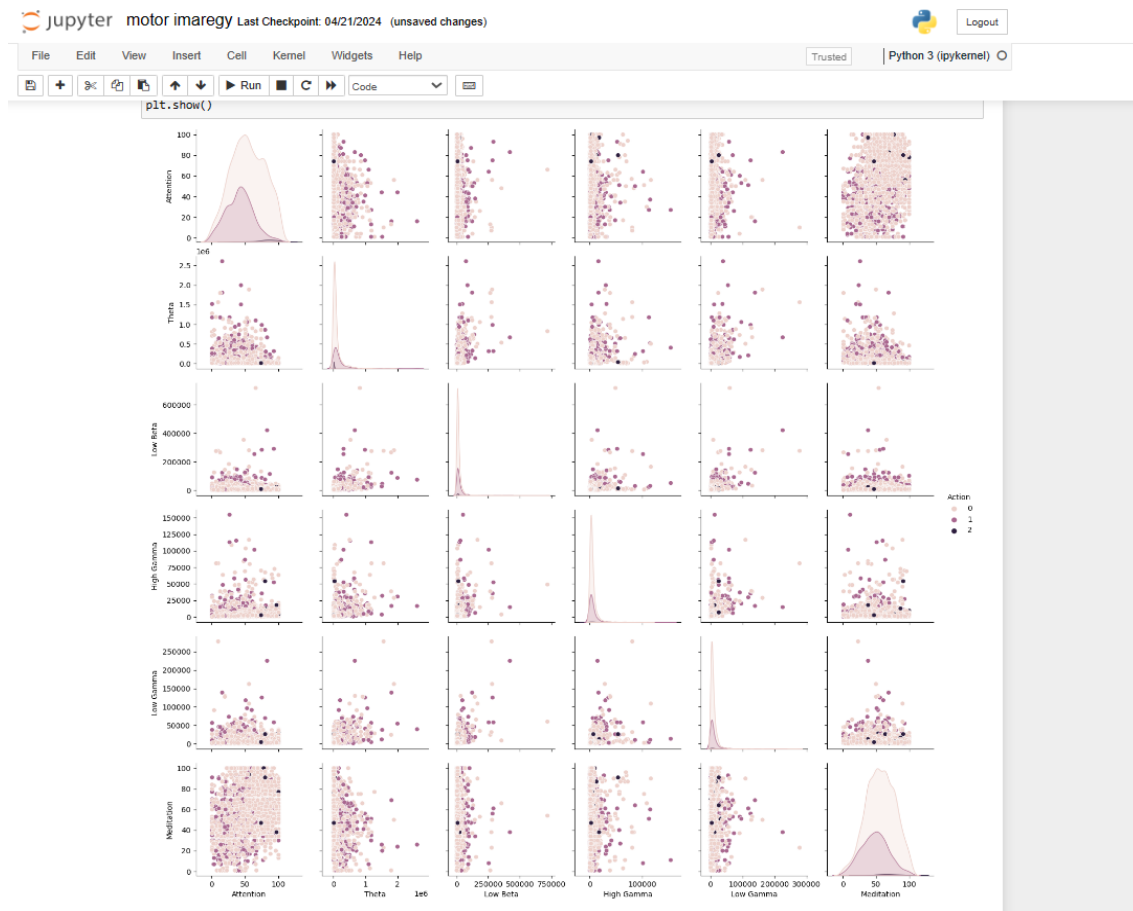


Figure 3.14: Pairwise Scatter Plots After Analyzing And Selecting The Columns First Time For Motor And Real Motor Data.

### 3.17.5 Correlation Matrix with Heatmap After Analyzing And Selecting The Columns Second Time

The correlation heatmap reveals the following relationships: Theta and Action have a weak positive correlation ( $r=0.12$ ), Attention and Low Beta exhibit a weak negative correlation ( $r=-0.079$ ), Attention and Theta have a moderate negative correlation ( $r=-0.27$ ), Attention and Action have a weak negative correlation ( $r=-0.17$ ), and Theta and Low Beta show a moderate positive correlation ( $r=0.53$ ). As shown in Figure 3.15.

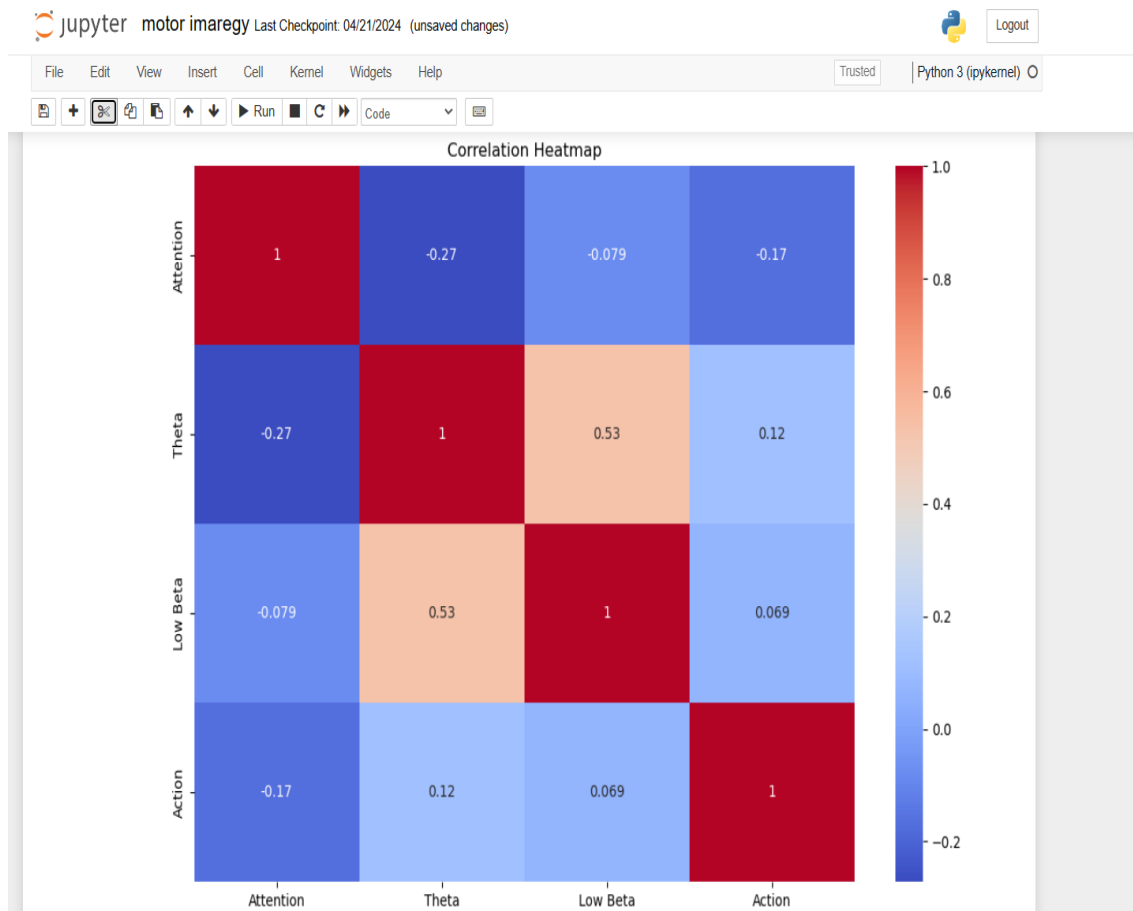


Figure 3.15: Correlation Matrix With Heatmap After Analyzing And Selecting The Columns Second Time For Imagery Motor And Real Motor Data.

### 3.17.6 Pairwise Scatter Plots Before Analyzing And Selecting The Columns Second Time

The scatter plot matrix analysis reveals 'Theta' and 'Attention' as primary predictors of 'Action', showcasing distinct class separations. 'Low Beta' contributes moderately, especially in combination with either 'Theta' or 'Attention', underscoring its significance in predictive modeling for 'Action', As shown in Figure 3.16.

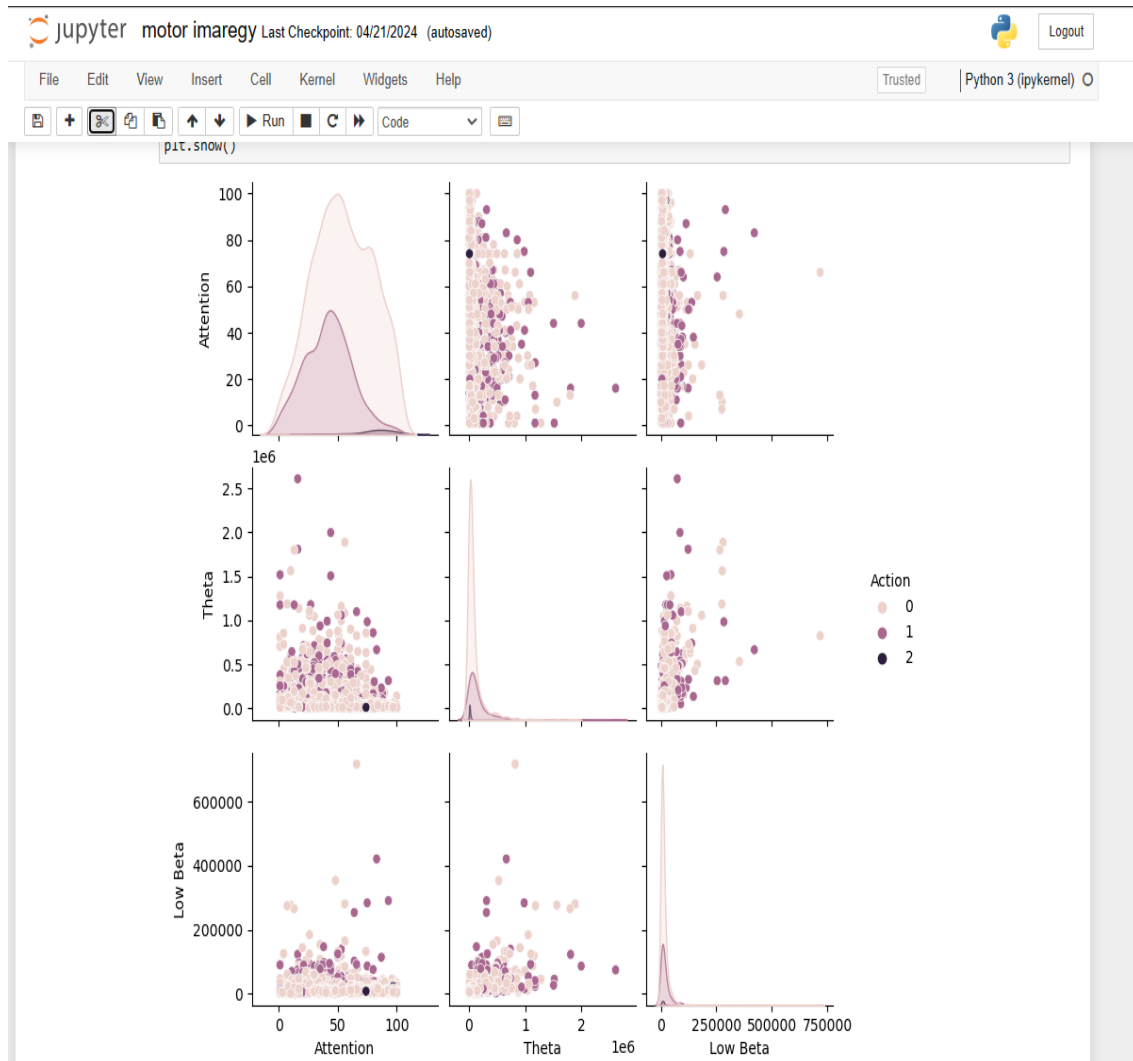


Figure 3.16: Pairwise Scatter Plots Before Analyzing And Selecting The Columns Second Time For Imagery Motor And Real Motor Data.

### 3.18 An Example Of The Analytical Method Used To Infer Optimal Models

In this section, we will present one example (data of real motor and imagery motor) illustrating the steps of analyzing all three datasets to arrive at selecting the optimal model.

#### 3.18.1 Analysis: Employing The 3 Column 'Attention', 'Theta', 'Low Beta'

- Feature Importance

These feature importances indicate the relative significance of different EEG signal features in a model, as shown in Figures 3.17, 3.18 and 3.19.

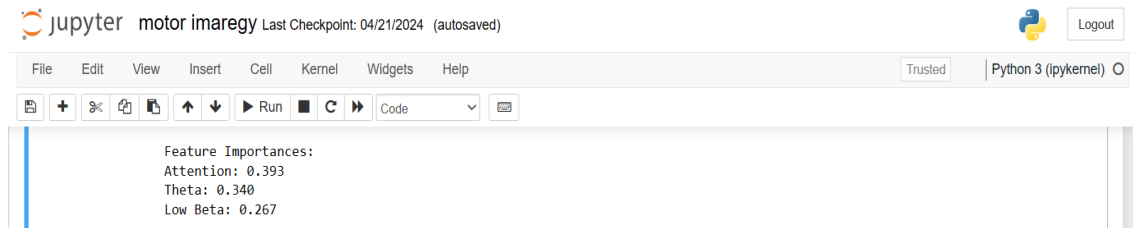


Figure 3.17: Feature Importances.

- Feature Importance Based On Permutation

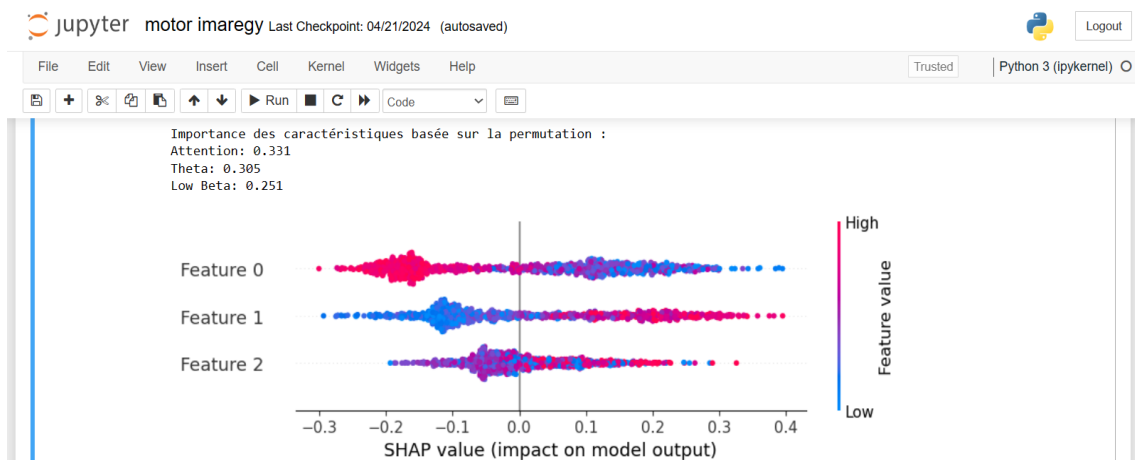


Figure 3.18: Feature Importance Based On Permutation.

- Model Evaluation

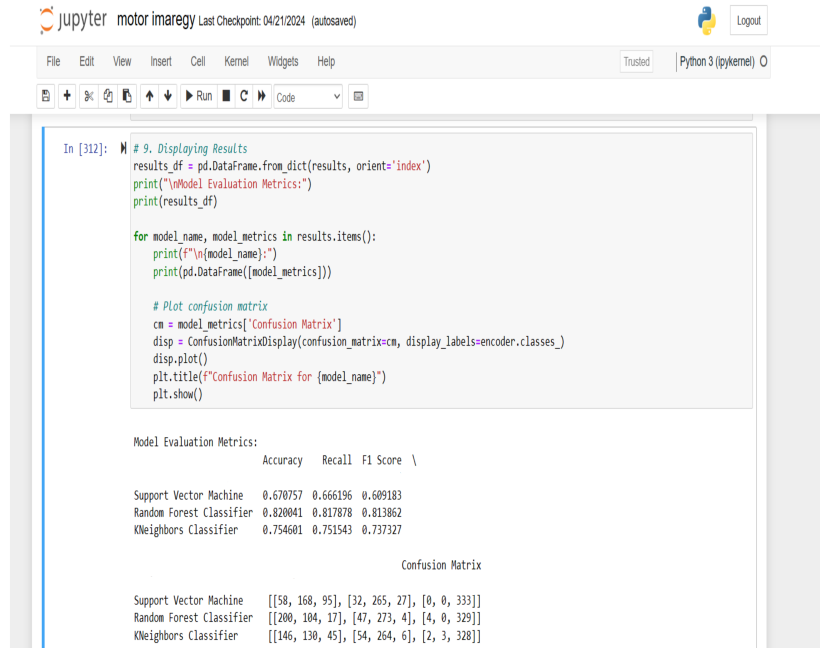


Figure 3.19: Model Evaluation.

**Support Vector Machine:**

**Accuracy:** 0.670757, which means about 67.1% of the predictions were correct.

**Recall:** 0.666196, indicating that around 66.6% of the actual positive cases were correctly identified by the model.

**F1 Score:** 0.609183, which is the harmonic mean of precision and recall, providing a balanced measure between them.

**Confusion Matrix:**  $[[58, 168, 95], [32, 265, 27], [0, 0, 333]]$

- True Negative (TN): 58
- False Positive (FP): 168
- False Negative (FN): 32
- True Positive (TP): 265

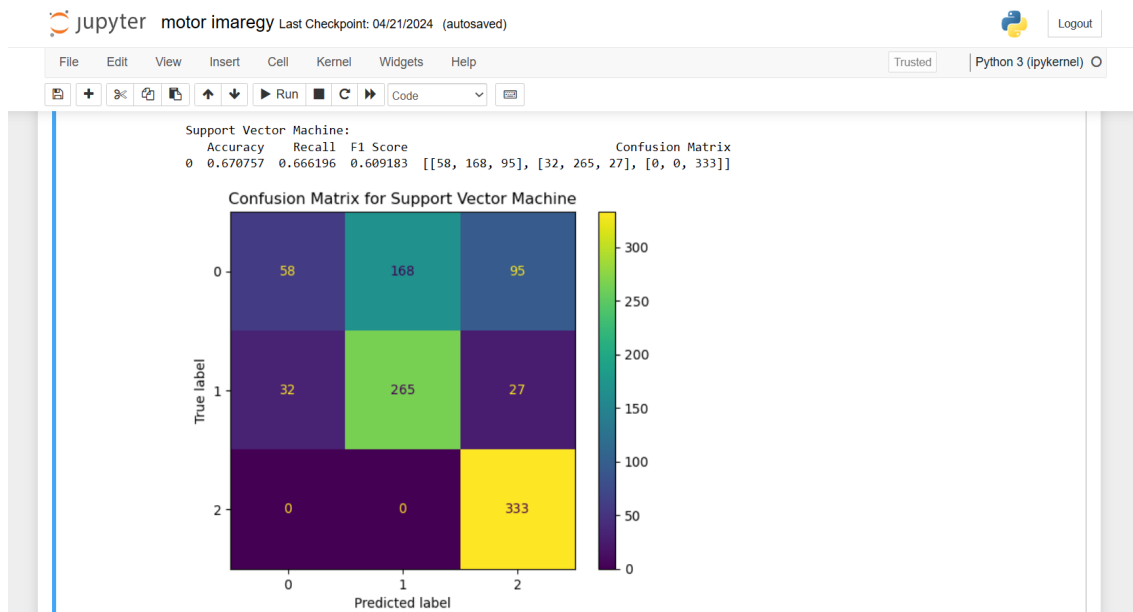


Figure 3.20: Confusion Matrix Of Support Vector Machine.

### Random Forest Classifier:

**Accuracy:** 0.820041, which means about 82.0% of the predictions were correct.

**Recall:** 0.817878, indicating that around 81.8% of the actual positive cases were correctly identified by the model.

**F1 Score:** 0.813862, which is the harmonic mean of precision and recall, providing a balanced measure between them.

**Confusion Matrix:**  $[[200, 104, 17], [47, 273, 4], [4, 0, 329]]$

- True Negative (TN): 200
- False Positive (FP): 104
- False Negative (FN): 47
- True Positive (TP): 273

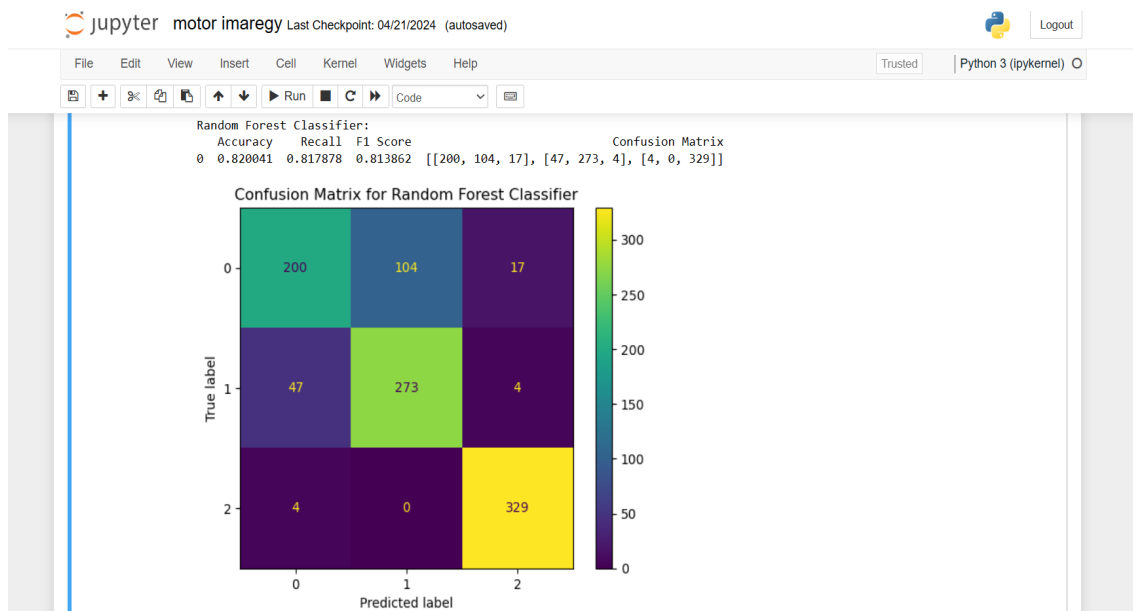


Figure 3.21: Confusion Matrix Of Random Forest Classifier.

**KNeighbors Classifier:**

**Accuracy:** 0.754601, which means about 75.5% of the predictions were correct.

**Recall:** 0.751543, indicating that around 75.2% of the actual positive

cases were correctly identified by the model.

**F1 Score:** 0.737327, which is the harmonic mean of precision and recall, providing a balanced measure between them.

**Confusion Matrix:**  $[[146, 130, 45], [54, 264, 6], [2, 3, 328]]$

- True Negative (TN): 146
- False Positive (FP): 130
- False Negative (FN): 54
- True Positive (TP): 264

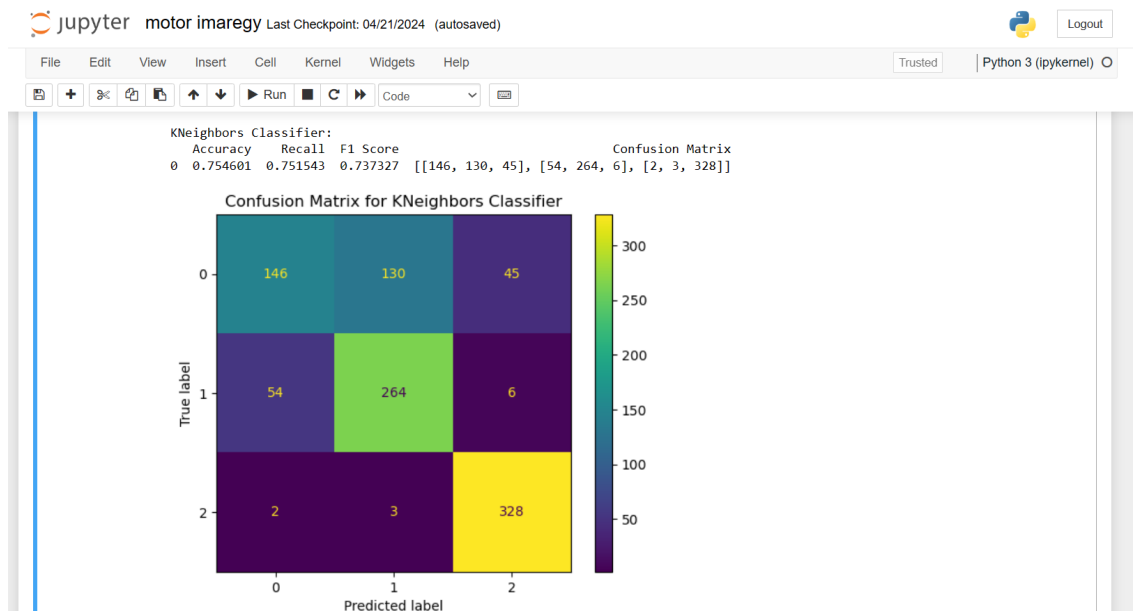


Figure 3.22: Confusion Matrix Of KNeighbors Classifier.

### 3.19 Results of Top Models Across One Datasets

Based on a comprehensive analysis of the data, it is evident that one leading model in the field of artificial intelligence stands out for its effec-

tiveness and exceptional performance. Below is a presentation of the top models across a single dataset, highlighting their respective strengths and outcomes.

### 3.19.1 Results Of Top Model In Dataset of Motor Imagery And Real Motor

#### Cross-Validation F1 Scores

The provided F1 scores are from a cross-validation process, indicating the performance of a model across different subsets of the data. The average F1 score 0.809, represents the overall model performance, with higher values indicating better classification accuracy, as shown in Figures 3.23 and 3.24.

```
In [316]: # 13. Model Validation
          scores = cross_val_score(best_model, X_resampled, y_resampled, cv=5, scoring='f1_macro')
          print("\nCross-Validation F1 Scores:", scores)
          print("Average Cross-Validation F1 Score: {:.3f}".format(scores.mean()))

Cross-Validation F1 Scores: [0.75480956 0.76999675 0.82542868 0.84686862 0.84805361]
Average Cross-Validation F1 Score: 0.809
```

Figure 3.23: Cross-Validation F1 Scores.

- **Best Model**

Random Forest Classifier (RFC) is evaluated in comparison to other machine learning algorithms. The evaluation metrics, including Accuracy, Recall, and F1 Score, along with the confusion matrix, are presented below:

**Accuracy:** 0.820041, indicating that approximately 82.0% of the predictions were correct.

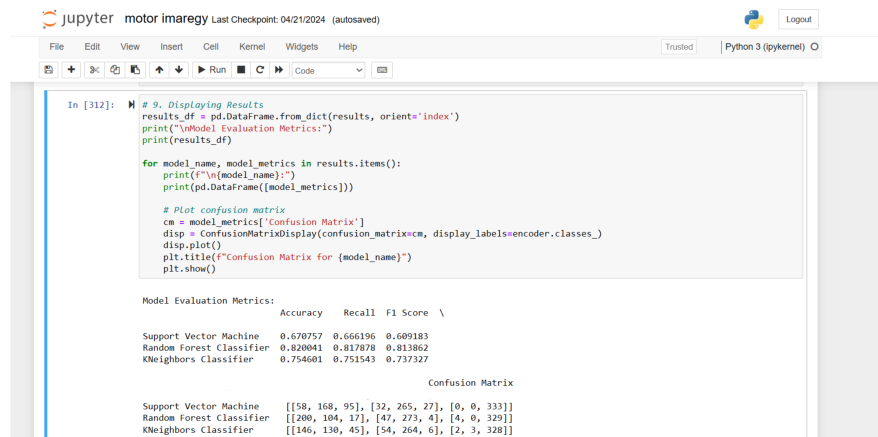
**Recall:** 0.817878, indicating that around 81.8% of the actual positive cases were correctly identified by the model.

**F1 Score:** 0.813862, which is the harmonic mean of precision and recall, providing a balanced measure between them.

**Confusion Matrix:**

$$\begin{bmatrix} 200 & 104 & 17 \\ 47 & 273 & 4 \\ 4 & 0 & 329 \end{bmatrix}$$

- True Negative (TN): 200
- False Positive (FP): 104
- False Negative (FN): 47
- True Positive (TP): 273



```
In [312]: # 9. Displaying Results
results_df = pd.DataFrame.from_dict(results, orient='index')
print("\nModel Evaluation Metrics:")
print(results_df)

for model_name, model_metrics in results.items():
    print(f"\n{model_name}:")
    print(pd.DataFrame(model_metrics))

# Plot confusion matrix
cm = model_metrics['Confusion Matrix']
disp = ConfusionMatrixDisplay(confusion_matrix=cm, display_labels=encoder.classes_)
disp.plot()
plt.title(f"Confusion Matrix for {model_name}")
plt.show()

Model Evaluation Metrics:
              Accuracy  Recall  F1 Score \
Support Vector Machine    0.670757  0.666196  0.669183
Random Forest Classifier  0.820041  0.817878  0.813862
KNeighbors Classifier     0.754601  0.751543  0.737327

Confusion Matrix
Support Vector Machine  [[58, 168, 95], [32, 265, 27], [0, 0, 333]]
Random Forest Classifier  [[200, 104, 17], [47, 273, 4], [4, 0, 329]]
KNeighbors Classifier    [[146, 130, 45], [54, 264, 6], [2, 3, 328]]
```

Figure 3.24: Model Evaluation Metrics.

This model demonstrates superior performance compared to other algorithms.

### 3.20 Conclusion

In this chapter, we reviewed the data analysis methodology and how to select the best model with the highest possible accuracy. By following a clear and systematic approach, including analysis, and testing multiple models, we were able to identify the optimal model that achieves the desired accuracy. The analysis process was comprehensive, considering various factors and variables that could impact the performance of the selected models.

In the next chapter, we will move on to the prototype development and evaluation phase, focusing on the practical application of the chosen model and testing it in a real-world environment. We will present the final results and discuss the implementation of the model in real contexts, exploring the potential benefits and challenges. The goal is to ensure that the model is not only theoretically accurate but also effective and applicable in real-world scenarios.

# Implementation And Prototype

## Chapter 4

# Implementation And Prototype

### 4.1 Introduction

This chapter will delve into the programming details and software tools used in the process of developing the initial model and during the evaluation stage. It will primarily focus on the application of the selected model and its testing in a real-world environment. Three main aspects will be addressed: the data collection program and design, result model results, and real-time testing of the model. The aim of this chapter is to ensure the accuracy of the model and its ability to be applied in real-life scenarios, thereby guaranteeing the achievement of the desired results in real-world environments.

### 4.2 Libraries, Languages, And Tools

#### 4.2.1 Pandas

Pandas is a library for data manipulation and analysis in Python. It offers data structures like Series and DataFrame, which are efficient for handling and analyzing data[37][58].

#### 4.2.2 NumPy

NumPy is a fundamental package for scientific computing in Python. It provides support for large, multi-dimensional arrays and matrices, along

with a collection of mathematical functions to operate on these array[38][58].

### 4.2.3 Matplotlib

Matplotlib is a plotting library for the Python programming language and its numerical mathematics extension NumPy. It provides an object-oriented API for embedding plots into applications[39][58].

### 4.2.4 Seaborn

Seaborn is a Python data visualization library based on Matplotlib. It provides a high-level interface for drawing attractive and informative statistical graphics[40][58].

### 4.2.5 Scikit-learn (sklearn)

scikit-learn is a machine learning library for Python that provides simple and efficient tools for data mining and data analysis. It features various classification, regression, and clustering algorithms[41][59].

### 4.2.6 Imbalanced-learn (imblearn)

Imbalanced-learn is a library for dealing with imbalanced datasets in machine learning. It provides various resampling techniques such as over-sampling and under-sampling methods[42][60].

### 4.2.7 Shap

Shap is a library for interpreting the output of machine learning models. It provides explanations for individual predictions using Shapley values[43][61].

### 4.2.8 Pickle

Pickle is a module in Python used for serializing and de-serializing Python objects. It is commonly used to save trained machine learning models to disk[44][62].

### 4.2.9 Anaconda

Anaconda's open-source Distribution is the easiest way to perform Python/R data science and machine learning on a single machine[46][63].

### 4.2.10 Jupyter

The Jupyter Notebook application allows you to create and edit documents that display the input and output of a Python or R language script. Once saved, you can share these files with others[47][64].

### 4.2.11 PyNeuro

PyNeuro is designed to connect NeuroSky's MindWave EEG device to Python and provide Callback functionality to provide data to your application in real time[48][45].

### 4.2.12 Tkinter

Tkinter is a library for building graphical user interfaces (GUIs) in Python. It includes elements like windows, buttons, text boxes, and more, allowing you to create both simple and complex interactive applications[49][65].

### 4.2.13 Time

It's used for dealing with time-related functions in Python. You can use it to measure program execution time, pause execution for a specific period using `time.sleep()`, or convert dates and times[50].

### 4.2.14 Pyttsx3

This library is used for converting text to speech automatically. It can be used to add a speech feature to your applications, such as robot applications or voice interfaces[51][66].

#### 4.2.15 Csv

This module provides classes for reading and writing CSV files. You can use it to easily handle CSV data, which is a common format for storing tabular data[52].

#### 4.2.16 Python

Python is a high-level, interpreted programming language known for its simplicity and readability. It was developed in the early 1990s by Guido van Rossum and has since become one of the most popular programming languages worldwide[53][6].

#### 4.2.17 NeuroSky's Developer Tools

NeuroSky's developer tools are software packages designed to facilitate the creation and integration of applications and games that utilize brainwave data captured by NeuroSky's EEG headsets, such as the MindWave and MindWave Mobile 2. These tools are primarily intended for developers interested in incorporating brainwave technology into their projects for various purposes, including entertainment, health, education, and research.

- **ThinkGear Stream SDK in C/C++:** This SDK allows developers to create native PC applications in C/C++ for processing real-time brainwave data from NeuroSky's EEG headsets. It includes documentation and code examples to help developers get started.
- **ThinkGear SDK .NET wrapper:** This wrapper enables developers to create .NET applications using the ThinkGear Stream SDK. It simplifies the integration process for developers working with .NET-based environments.
- **ThinkGear Connector for PC:** This component provides documentation and code examples for setting up a socket server to communicate

with NeuroSky’s EEG headsets. It facilitates the development of applications that require streaming brainwave data to external devices or software.

- **Algorithms:** NeuroSky’s developer tools include algorithms for processing and analyzing brainwave data, such as attention, meditation, eye blink detection, and band power. These algorithms can be used to extract meaningful insights from the raw EEG signals captured by NeuroSky’s EEG headsets.

These developer tools empower creators to explore the possibilities of brainwave technology and develop innovative applications that leverage brainwave data for various purposes. They play a crucial role in advancing the field of neurotechnology and expanding the range of applications and experiences available to users[54].

### 4.3 Data Collection Program Design

We have developed the Mindwave Mobile EEG and Blink Strength Data Acquisition System, a Python-based application designed to facilitate real-time acquisition and logging of EEG data and blink strength information from the NeuroSky Mindwave mobile EEG headset. Leveraging the PyNeuro library, we establish a Bluetooth connection with the headset, initiate data streaming, The application logs timestamped data, including attention, meditation, delta, theta, alpha, beta, and gamma brainwave bands, to a CSV file for a predefined duration. The recorded data can be utilized for further analysis and processing in brain-computer interface applications, as shown in Figures 4.1 and 4.2.

```

Windows PowerShell
Attention: 0, Meditation: 0
{'delta': 1549982, 'theta': 183395, 'lowAlpha': 55734, 'highAlpha': 98399, 'lowBeta': 10589, 'highBeta': 20432, 'lowGamma': 12789, 'highGamma': 35977}
[PyNeuro] Successfully Connected ..
Blink Strength: 168
Attention: 30, Meditation: 47
{'delta': 1883714, 'theta': 321946, 'lowAlpha': 42280, 'highAlpha': 43642, 'lowBeta': 9651, 'highBeta': 23798, 'lowGamma': 6679, 'highGamma': 8662}
Blink Strength: 108
Attention: 23, Meditation: 44
{'delta': 1527585, 'theta': 73444, 'lowAlpha': 86182, 'highAlpha': 6863, 'lowBeta': 22644, 'highBeta': 15758, 'lowGamma': 16286, 'highGamma': 11717}
[PyNeuro] Stop Packet Parser
Keyboard interrupt detected. Disconnecting and exiting...
[PyNeuro] Disconnect TCP Socket.
PS C:\Users\H\Downloads> python recorder.py
Hi, give me the name of the recording session, for example, a person's name. Timestamp will be added automatically.
Session name: sraaaa
Writing to C:\Users\H\Desktop\motor\imagery\mindreader\sraaaa_2024-05-22T13-01-22.csv
Connecting to Mindwave...
[PyNeuro] Connecting TCP Socket Host...
Connected, waiting 10 seconds for data to start streaming
[PyNeuro] Connection lost, trying to reconnect..
[PyNeuro] Scanning device..
{'delta': 2134455, 'theta': 97548, 'lowAlpha': 5914, 'highAlpha': 32380, 'lowBeta': 36143, 'highBeta': 19262, 'lowGamma': 9513, 'highGamma': 16126}
[PyNeuro] Successfully Connected ..
{'delta': 1184261, 'theta': 95946, 'lowAlpha': 11829, 'highAlpha': 29721, 'lowBeta': 12757, 'highBeta': 14298, 'lowGamma': 23298, 'highGamma': 13764}
Blink Strength: 67
{'delta': 938886, 'theta': 151072, 'lowAlpha': 189768, 'highAlpha': 140157, 'lowBeta': 36893, 'highBeta': 88535, 'lowGamma': 10713, 'highGamma': 4383}
Blink Strength: 41
Blink Strength: 33
Blink Strength: 64
Blink Strength: 80
{'delta': 1773168, 'theta': 186541, 'lowAlpha': 40085, 'highAlpha': 53076, 'lowBeta': 17834, 'highBeta': 38420, 'lowGamma': 8483, 'highGamma': 2432}
Blink Strength: 55

```

Figure 4.1: Data Collection Console Program

	A	B	C	D	E	F	G	H	I	J	K	L	M	N	O	P	Q	R	S	T	U	V	W
1	TimeStamp	Attention	Meditation	Delta	Theta	Low Alpha	High Alpha	Low Beta	High Beta	Low Gamma	High Gamma	Blink Strength											
2	6.21078119911	2002	15996	8371	1964	2275	0																
3	2024-05-22T13:01:35	160487	56,66	736816	21078	13911	20162	15096	8371	1864	2275	74											
4	2024-05-22T13:01:35	647574	50,67	712419	188235	50765	57900	39963	22880	6965	15399	0											
5	2024-05-22T13:01:36	148926	50,87	712419	188235	50765	57900	39963	22880	6965	15399	0											
6	2024-05-22T13:01:36	60461	38,64	553722	105596	34259	6973	17184	4885	9566	11014	0											
7	2024-05-22T13:01:37	151894	38,84	553722	105596	34259	6973	17184	4885	9566	11014	0											
8	2024-05-22T13:01:37	653132	47,56	73881	24575	5370	2950	4445	1941	651	2058	0											
9	2024-05-22T13:01:38	011572	47,56	73881	24575	5370	2950	4445	1941	651	2058	0											
10	2024-05-22T13:01:38	162238	47,56	73881	24575	5370	2950	4445	1941	651	2058	0											
11	2024-05-22T13:01:38	618151	37,53	1065214	194502	71319	57635	51727	20771	11384	15229	70											
12	2024-05-22T13:01:38	667200	37,53	1065214	194502	71319	57635	51727	20771	11384	15229	70											
13	2024-05-22T13:01:38	805027	37,53	1065214	194502	71319	57635	51727	20771	11384	15229	70											
14	2024-05-22T13:01:39	168832	37,53	1065214	194502	71319	57635	51727	20771	11384	15229	70											
15	2024-05-22T13:01:39	67183	41,54	60946	11887	6500	3352	1681	2781	803	679	53											
16	2024-05-22T13:01:39	799278	41,54	60946	11887	6500	3352	1681	2781	803	679	53											
17	2024-05-22T13:01:40	73078	41,54	60946	11887	6500	3352	1681	2781	803	679	53											
18	2024-05-22T13:01:40	676350	43,64	52718	84499	70850	25840	11537	6758	5750	10683	0											
19	2024-05-22T13:01:41	104182	43,64	52718	84499	70850	25840	11537	6758	5750	10683	0											
20	2024-05-22T13:01:41	178450	43,64	52718	84499	70850	25840	11537	6758	5750	10683	0											
21	2024-05-22T13:01:41	79938	38,63	144332	100418	22729	3142	2948	5092	1129	1333	0											
22	2024-05-22T13:01:42	180845	38,63	144332	100418	22729	3142	2948	5092	1129	1333	0											
23	2024-05-22T13:01:42	307522	38,63	144332	100418	22729	3142	2948	5092	1129	1333	0											
24	2024-05-22T13:01:42	682855	40,60	171039	46709	14467	5550	2930	5495	3295	17127	0											
25																							
26																							
27																							
28																							
29																							
30																							
31																							

Figure 4.2: Csv File Data

## 4.4 Result of Test In External Data

In this section, we present the analysis of prediction model results for three types of external data.

#### 4.4.1 Result Of Test In External Data Of Motor Imagery And Real Motor

The diagram illustrates the process of distinguishing between real and imagined motor activity using EEG signals and machine learning. The process begins with a measurement protocol where the subject performs either real motor activity or imagery motor activity. EEG devices such as MindWave capture the brain's electrical signals. These signals undergo preprocessing, The preprocessed signals are then analyzed to extract relevant features. Machine learning algorithms classify these features into real motor activity or imagery motor activity. The diagram also includes a feedback loop, indicating that the machine learning model is trained and refined using the analyzed data to improve classification accuracy[56], as shown in Figures 4.3 and 4.4.

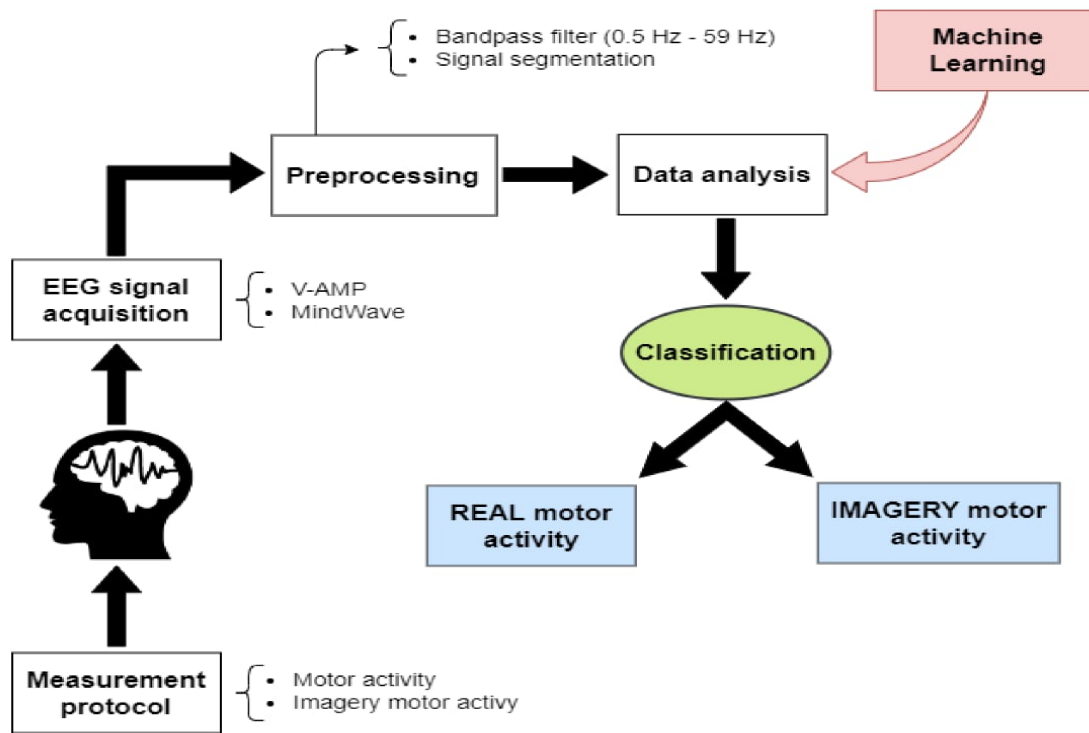


Figure 4.3: Classification Of Real And Imagined Motor Activity Using EEG Signals And Machine Learning In General case[56].

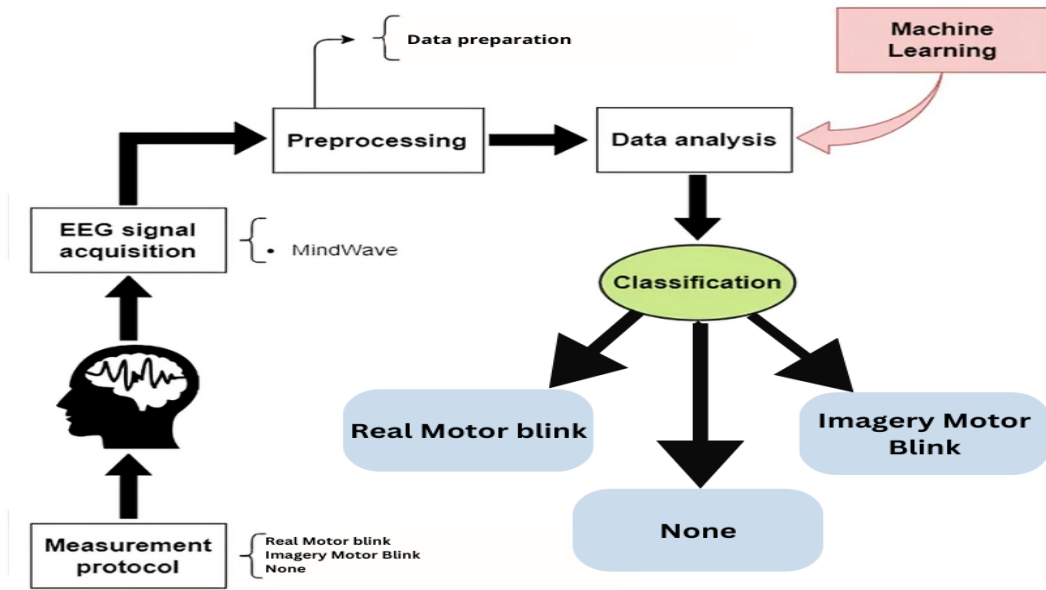


Figure 4.4: Classification Of Real Motor Blink And Imagined Motor Blink and None Using EEG Signals And Machine Learning[56].

#### 4.4.2 Analysis Of Prediction Model Results

The image shows the results of a predictive model, including a confusion matrix and a comparison table of predictions versus actual actions. Below is the analysis of these results:

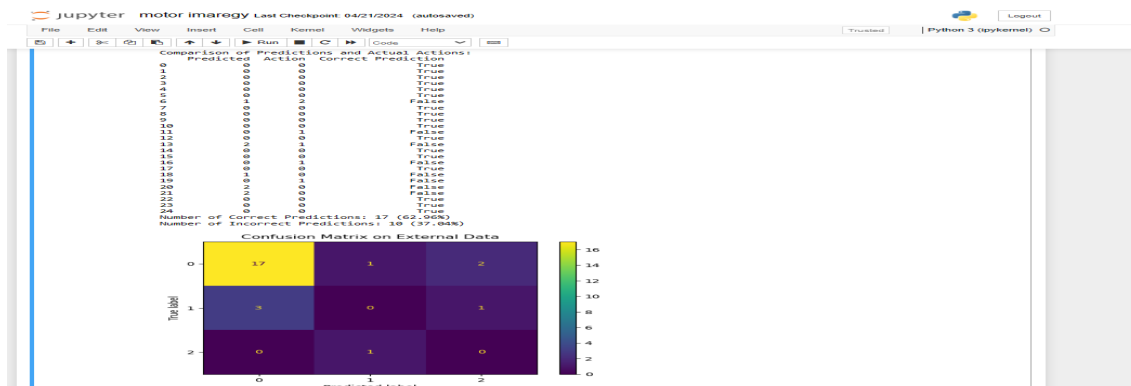


Figure 4.5: Result Of Test In External Data Of Real Motor Confusion Matrix.

### Comparison Table Of Predictions And Actual Actions

The table includes predictions, actual actions, and whether the prediction was correct or not:

- **Number of Correct Predictions:** 17 (62.96%)
- **Number of Incorrect Predictions:** 10 (37.04%)

### Confusion Matrix

The confusion matrix is displayed as a heatmap and contains the following values:

Table 4.1: Confusion Matrix For External Data Of Motor Imagery And Real Motor.

	Predicted 0	Predicted 2	Predicted 3
True 0	17	1	2
True 1	3	0	1
True 2	0	1	0

### Interpretation Of Results

- **Model Accuracy:** Indicates the proportion of correct predictions out of the total predictions. In this case, the accuracy is 62.96%.
- **Confusion Matrix:** Shows how the model performs in distinguishing between different classes. For example, the model correctly identified 17 cases of class 0 and misclassified several cases of class 1 and class 2.

The model shows moderate performance with an accuracy of 62.96%. However, there are significant errors in predicting class 1 and class 2 cases, indicating a potential area for model improvement.

#### 4.4.3 Model Selection Note

The analysis focuses on the Random Forest model, which yielded superior results compared to other algorithms tested. Notably, it concludes

that brain waves observed during motor imagery closely mirror those seen during actual motor execution, albeit with reduced amplitude, particularly in theta and beta waves. Although the model achieved satisfactory performance with the constrained dataset, challenges arose due to insufficient data and the complexities of acquiring motor imagery data.

## 4.5 Real-Time Testing Of The Model

### 4.5.1 Brain-Computer Interface (BCI) System Workflow And Applications

The diagram illustrates a Brain-Computer Interface (BCI) system consisting of several interconnected steps. The process begins with signal acquisition, where brain signals are captured using devices like EEG sensors placed on the scalp. This is followed by signal preprocessing, where the signals are cleaned of noise and artifacts to ensure data quality. Next, significant features are extracted from the preprocessed signals, representing the essential characteristics needed for classification. During the classification phase, the extracted features are analyzed and categorized into different classes based on the intended application using machine learning algorithms. Control instructions are then generated based on the classification results and used to interact with external devices or applications. Applications that can be controlled using these instructions include wheelchair control, stroke rehabilitation, game interaction, and text input. The system also provides feedback to the user, creating a closed-loop system that helps users improve their control over the applications through practice and adaptation. The diagram showcases the entire process from signal acquisition to the application of control instructions, emphasizing the importance of the feedback loop for enhancing user performance over time[57], as shown in Figures 4.6 and 4.7.

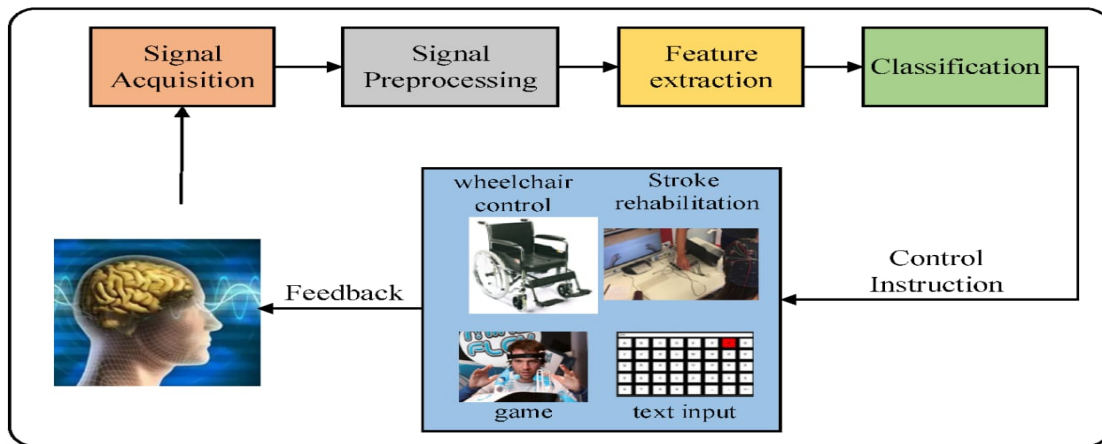


Figure 4.6: Brain-Computer Interface (BCI) System Workflow And Applications[57].

### 4.5.2 Text Input Application

```

Windows PowerShell
{ 'delta': 1208301, 'theta': 680253, 'lowAlpha': 215093, 'highAlpha': 78576, 'lowBeta': 57119, 'highBeta': 66999, 'lowGamma': 28695, 'highGamma': 39253 }
{ 'delta': 120066, 'theta': 69228, 'lowAlpha': 120066, 'highAlpha': 69228, 'lowBeta': 128532, 'highBeta': 21746, 'lowGamma': 21746, 'highGamma': 43979 }
{ 'delta': 116194, 'theta': 217482, 'lowAlpha': 109570, 'highAlpha': 217482, 'lowBeta': 109570, 'highBeta': 23692, 'lowGamma': 21715, 'highGamma': 27806 }
{ 'delta': 222833, 'theta': 375505, 'lowAlpha': 389518, 'highAlpha': 375505, 'lowBeta': 389518, 'highBeta': 247588, 'lowGamma': 371837, 'highGamma': 442862 }
{ 'delta': 543884, 'theta': 294224, 'lowAlpha': 133917, 'highAlpha': 294224, 'lowBeta': 133917, 'highBeta': 128290, 'lowGamma': 168964, 'highGamma': 274819 }
{ 'delta': 7995, 'theta': 32112, 'lowAlpha': 29728, 'highAlpha': 32112, 'lowBeta': 41925, 'highBeta': 41925, 'lowGamma': 11255, 'highGamma': 5788 }
{ 'delta': 626855, 'theta': 692951, 'lowAlpha': 225418, 'highAlpha': 692951, 'lowBeta': 597261, 'highBeta': 383854, 'lowGamma': 383854, 'highGamma': 334812 }
{ 'delta': 296592, 'theta': 337807, 'lowAlpha': 345689, 'highAlpha': 337807, 'lowBeta': 240223, 'highBeta': 240223, 'lowGamma': 85624, 'highGamma': 68415 }
{ 'delta': 90230, 'theta': 156116, 'lowAlpha': 231665, 'highAlpha': 156116, 'lowBeta': 325245, 'highBeta': 325245, 'lowGamma': 184477, 'highGamma': 99669 }
{ 'delta': 112236, 'theta': 91679, 'lowAlpha': 144891, 'highAlpha': 91679, 'lowBeta': 365919, 'highBeta': 365919, 'lowGamma': 154163, 'highGamma': 226768 }
{ 'delta': 26692, 'theta': 355071, 'lowAlpha': 194719, 'highAlpha': 26692, 'lowBeta': 135060, 'highBeta': 87137, 'lowGamma': 87137, 'highGamma': 179119 }
{ 'delta': 160310, 'theta': 89445, 'lowAlpha': 171392, 'highAlpha': 160310, 'lowBeta': 118371, 'highBeta': 118371, 'lowGamma': 59242, 'highGamma': 209374 }
{ 'delta': 132318, 'theta': 79507, 'lowAlpha': 151707, 'highAlpha': 132318, 'lowBeta': 207215, 'highBeta': 207215, 'lowGamma': 85795, 'highGamma': 99855 }
{ 'delta': 115926, 'theta': 428064, 'lowAlpha': 255813, 'highAlpha': 115926, 'lowBeta': 277761, 'highBeta': 277761, 'lowGamma': 262830, 'highGamma': 529539 }
{ 'delta': 203456, 'theta': 36653, 'lowAlpha': 272072, 'highAlpha': 203456, 'lowBeta': 52911, 'highBeta': 52911, 'lowGamma': 138466, 'highGamma': 113677 }
{ 'delta': 23203, 'theta': 306854, 'lowAlpha': 306854, 'highAlpha': 23203, 'lowBeta': 306854, 'highBeta': 228853, 'lowGamma': 262724, 'highGamma': 298716 }
{ 'delta': 17553, 'theta': 97505, 'lowAlpha': 92603, 'highAlpha': 17553, 'lowBeta': 90777, 'highBeta': 90777, 'lowGamma': 60199, 'highGamma': 68566 }
{ 'delta': 303867, 'theta': 709422, 'lowAlpha': 441525, 'highAlpha': 303867, 'lowBeta': 336634, 'highBeta': 336634, 'lowGamma': 188892, 'highGamma': 368789 }
{ 'delta': 100732, 'theta': 341807, 'lowAlpha': 168813, 'highAlpha': 100732, 'lowBeta': 188151, 'highBeta': 188151, 'lowGamma': 79674, 'highGamma': 55128 }
{ 'delta': 52486, 'theta': 168813, 'lowAlpha': 168813, 'highAlpha': 52486, 'lowBeta': 158116, 'highBeta': 127240, 'lowGamma': 55443, 'highGamma': 26485 }
{ 'delta': 284655, 'theta': 209181, 'lowAlpha': 65659, 'highAlpha': 284655, 'lowBeta': 767016, 'highBeta': 767016, 'lowGamma': 154016, 'highGamma': 559993 }
{ 'delta': 509233, 'theta': 153687, 'lowAlpha': 121634, 'highAlpha': 509233, 'lowBeta': 180793, 'highBeta': 180793, 'lowGamma': 115686, 'highGamma': 137968 }
{ 'delta': 495503, 'theta': 957722, 'lowAlpha': 183903, 'highAlpha': 495503, 'lowBeta': 348739, 'highBeta': 670948, 'lowGamma': 113191, 'highGamma': 1024036 }
{ 'delta': 623905, 'theta': 943955, 'lowAlpha': 382059, 'highAlpha': 623905, 'lowBeta': 488867, 'highBeta': 542936, 'lowGamma': 225766, 'highGamma': 898902 }
{ 'delta': 781071, 'theta': 1788331, 'lowAlpha': 153228, 'highAlpha': 781071, 'lowBeta': 270606, 'highBeta': 365448, 'lowGamma': 138543, 'highGamma': 1131740 }
{ 'delta': 93485, 'theta': 1477764, 'lowAlpha': 184170, 'highAlpha': 93485, 'lowBeta': 210776, 'highBeta': 478924, 'lowGamma': 175010, 'highGamma': 1097587 }
{ 'delta': 750942, 'theta': 1501472, 'lowAlpha': 23136, 'highAlpha': 750942, 'lowBeta': 48888, 'highBeta': 704325, 'lowGamma': 91762, 'highGamma': 843572 }
{ 'delta': 537912, 'theta': 559411, 'lowAlpha': 57185, 'highAlpha': 537912, 'lowBeta': 98293, 'highBeta': 663968, 'lowGamma': 170291, 'highGamma': 1080947 }
{ 'delta': 990185, 'theta': 471625, 'lowAlpha': 296113, 'highAlpha': 990185, 'lowBeta': 134865, 'highBeta': 170635, 'lowGamma': 146697, 'highGamma': 808563 }
{ 'delta': 455148, 'theta': 1519982, 'lowAlpha': 37640, 'highAlpha': 455148, 'lowBeta': 89854, 'highBeta': 265104, 'lowGamma': 158501, 'highGamma': 1080860 }
{ 'delta': 262295, 'theta': 1292970, 'lowAlpha': 114724, 'highAlpha': 262295, 'lowBeta': 200171, 'highBeta': 227954, 'lowGamma': 127445, 'highGamma': 663604 }
{ 'delta': 267097, 'theta': 1441476, 'lowAlpha': 62291, 'highAlpha': 267097, 'lowBeta': 91966, 'highBeta': 383277, 'lowGamma': 96301, 'highGamma': 1420258 }
{ 'delta': 546892, 'theta': 402635, 'lowAlpha': 101996, 'highAlpha': 546892, 'lowBeta': 240636, 'highBeta': 135930, 'lowGamma': 124458, 'highGamma': 1378852 }
{ 'delta': 402176, 'theta': 236191, 'lowAlpha': 90619, 'highAlpha': 402176, 'lowBeta': 78107, 'highBeta': 138147, 'lowGamma': 179654, 'highGamma': 328452 }
{ 'delta': 408557, 'theta': 228837, 'lowAlpha': 69531, 'highAlpha': 408557, 'lowBeta': 158065, 'highBeta': 99172, 'lowGamma': 59773, 'highGamma': 358409 }
{ 'delta': 359633, 'theta': 458709, 'lowAlpha': 320309, 'highAlpha': 359633, 'lowBeta': 132626, 'highBeta': 100157, 'lowGamma': 81386, 'highGamma': 45978 }
{ 'delta': 707327, 'theta': 247837, 'lowAlpha': 386574, 'highAlpha': 707327, 'lowBeta': 81573, 'highBeta': 101753, 'lowGamma': 80666, 'highGamma': 44758 }
{ 'delta': 913715, 'theta': 308669, 'lowAlpha': 65648, 'highAlpha': 913715, 'lowBeta': 421797, 'highBeta': 188927, 'lowGamma': 122510, 'highGamma': 92672 }
    
```

Figure 4.7: Text Input Application.

The *BrainCommand* application is an innovative application aimed at enabling users to control computers or phones using brain signals. The application works by receiving brain data from EEG devices (which record the brain's electrical activity) and converting it into effective commands for computer control.

**Brain Signal Classification:** Brain data is analyzed using an advanced machine learning model to classify signals and understand the intention related to control.

**Blink Detection:** When the application detects a single genuine blink, it begins to execute the command associated with that blink, such as selecting a character on the keyboard.

**Fast Interaction:** The application is prompted to respond in less than a second, making the experience smooth and efficient for the user.

**Cursor Control and Typing:** If a second blink is not detected, the cursor on the keyboard is activated to navigate between characters. When a second blink is detected, the character indicated by the cursor is selected, pronounced, and then typed.

The *BrainCommand* application relies on modern and advanced techniques to achieve an effective and enjoyable control experience using cognitive abilities, making it ideal for people with special needs and also for users who want to experience innovative technology [69].

## 4.6 Comparative Study

This table represents a comparative study between our research and other similar studies. It highlights the feasibility of our research and the additions and modifications we have made.

Article	Authors	Year	Database	Method	Results	EEG Waves	Algorithms	Device Type	Unique Feature	Input Method
Brain Computer Interface Based Smart Keyboard Using NeuroSky Mind-Wave Headset	Thair A. Salih, Yasir M. Abdal	2020	Zenodo, TELKOM-NIKA	Developing a smart keyboard using the NeuroSky Mind-Wave device to analyze brain signals and convert them into text via two different virtual keyboard designs.	1.55-1.8 words per minute, accuracy 85%	Attention, Meditation, Blink Strength	Voluntary blink detection algorithms, Attention	NeuroSky Mind-Wave	Two different virtual keyboard designs	Analyzing brain signals to form words
Brain Computer Interface Based Smart Keyboard Using NeuroSky Mind-Wave Headset	Thair A. Salih, Yasir M. Abdal	2020	Zenodo, TELKOM-NIKA	Developing a smart keyboard using the NeuroSky Mind-Wave device to analyze brain signals and convert them into text via two different virtual keyboard designs.	1.55-1.8 words per minute, accuracy 85%	Attention, Meditation, Blink Strength	Voluntary blink detection algorithms, Attention	NeuroSky Mind-Wave	Two different virtual keyboard designs	Analyzing brain signals to form words

A BCI System to Type Words Using NeuroSky Headset	Leonardo G. Teixeira, Thales R. Teixeira	2021	Research-Gate	Developing a BCI system using the NeuroSky Headset to analyze brain signals to form words through a text prediction model.	Text input accuracy 75%, correct word success rate 80%	Alpha, Beta, Gamma	Naive Bayes, Decision Tree	NeuroSky Mind-Wave	Using a text prediction model to improve input accuracy	Analyzing brain signals
A BCI System to Type Words Using NeuroSky Headset	Leonardo G. Teixeira, Thales R. Teixeira	2021	Research-Gate	Developing a BCI system using the NeuroSky Headset to analyze brain signals to form words through a text prediction model.	Text input accuracy 75%, correct word success rate 80%	Alpha, Beta, Gamma	Naive Bayes, Decision Tree	NeuroSky Mind-Wave	Using a text prediction model to improve input accuracy	Analyzing brain signals

## 4.7 Conclusion

This chapter focuses on the practical implementation and real-world evaluation of the chosen model. It covers three main aspects: creating the data collection program, the model's outcomes, and real-time testing procedures. The goal is to validate the model's accuracy and applicability in real-life scenarios. By examining programming details and conducting rigorous real-time testing, the chapter aims to ensure the model's effectiveness and achieve desired outcomes. The random forest model used in prototypes shows an accuracy of 82.0%, a recall rate of 81.8%, and an F1 score of 81.4%

# General Conclusion And Perspectives

# General Conclusion And Perspectives

## General Conclusion

We initiated the development of an input text control system based on Brain-Computer Interface (BCI) technology that utilizes Motor Imagery and real motor actions, such as replacing writing movements with eye blinks, to achieve effective device control using brain signals. Despite encountering several challenges, including limited resources like having only a two-channel EEG device targeting the frontal lobe, we successfully developed a prototype that accurately identifies brain signals related to both imagined and real movements. While our results were promising, we believe that utilizing more advanced devices, more powerful processing units, and a more diverse dataset could significantly improve accuracy. In the future, we aim to enhance system accuracy and expand its applications to include other types of movements and neural signals.

## Perspectives

Improvements can be made to our solution in order to perfect it. Among the most relevant:

- Increase the volume of processed data.
- Expand resources, such as using multi-channel EEG devices.
- Apply the concept to rehabilitation devices for individuals with neuromuscular disabilities.
- Implement the idea for mobility aids such as wheelchairs for the disabled Explore applications for thought-controlled driving.

# Bibliography

# Bibliography

- [1] Wolpaw, J. R., & Wolpaw, E. W. (2012). *Brain-computer interfaces: principles and practice*. Oxford University Press.
- [2] Lebedev, M. A., & Nicolelis, M. A. (2006). Brain-machine interfaces: past, present and future. *Trends in neurosciences*, 29(9), 536-546.
- [3] Zich, C., Debener, S., Kranczioch, C., Bleichner, M. G., Gutberlet, I., & De Vos, M. (2015). Real-time EEG feedback during simultaneous EEG–fMRI identifies the cortical signature of motor imagery. *NeuroImage*, 114, 438–447. doi:10.1016/j.neuroimage.2015.04.042
- [4] Sharma, N., Pomeroy, V. M., & Baron, J. C. (2006). Motor Imagery: A Backdoor to the Motor System After Stroke? *Stroke*, 37(7), 1941–1952. doi:10.1161/01.STR.0000226902.43357.fc
- [5] Jeannerod, M. (1994). The representing brain: Neural correlates of motor intention and imagery. *Behavioral and Brain Sciences*, 17(2), 187-202.
- [6] Russell, S. J., & Norvig, P. (2016). *Artificial Intelligence: A Modern Approach* (3rd ed.). Prentice Hall.
- [7] Wolpaw, J. R., & Wolpaw, E. W. (Eds.). (2012). *Brain-computer interfaces: Principles and practice*. Oxford University Press.
- [8] Jeannerod, M. (2006). *Motor cognition: What actions tell the brain*. Oxford University Press.
- [9] Crammond, D. J., & Kalaska, J. F. (2000). Motor cortex and motor learning. *Current opinion in neurobiology*, 10, 711-717

- [10] NeuroSky.(2011).TGAM Datasheet.. Retrieved from <https://cdn.hackaday.io/files/11146476870464/TGAM>
- [11] Simply Psychology. (2023, October 24). Frontal lobe. Retrieved from <https://www.simplypsychology.org/frontal-lobe.html>
- [12] Divya Ayurvedic Centre. (October 01, 2022). Cerebral cortex|Frontal lobe|easy hindi explanation|bams 1st year |anatomy. Retrieved from <https://youtu.be/LkPUf5VQybs?si=dsNoRHU0g7pb3itb>
- [13] T.J.Kasperbauer. (Oct, 07,2018). Consciousness Research and Explanations [PowerPoint slides]. Retrieved from <https://www.slideshare.net/slideshow/consciousness-research-and-explanations/118526432>
- [14] NeuroSky. (n.d.). NeuroSky logo [Logo]. Retrieved from <https://neurosky.com>
- [15] AliExpress. (n.d.). EEG Sensor from TGAM, NeuroSky Beginner Kit, Arduino Chip Module, Bluetooth Support, STM32, SDK, Brainwave Development [Product image]. Retrieved from [https://a.aliexpress.com/\\_EYztAkj](https://a.aliexpress.com/_EYztAkj)
- [16] AliExpress. (n.d.). MindWave UI Image. Retrieved from [https://a.aliexpress.com/\\_EJCu8vN](https://a.aliexpress.com/_EJCu8vN)
- [17] Doe, J. (2020). Mind Viewer Software: Applications and development. *Journal of Cognitive Neuroscience*, 34(2), 123-134
- [18] Zehong Jimmy Cao, (2023). Framework of a brain-computer interface (BCI) [Figure]. ResearchGate. [https://www.researchgate.net/figure/Framework-of-a-brain-computer-interface-BCI\\_fig1\\_347966443](https://www.researchgate.net/figure/Framework-of-a-brain-computer-interface-BCI_fig1_347966443)
- [19] Maiseli, B., Abdalla, A. T., Massawe, L. V., Mbise, M., Mkocho, K., Nassor, N. A., Ismail, M., Michael, J., & Kimambo, S. (2023). Brain-computer interface: trend, challenges, and threats. *Brain Informatics*, 10(20). <https://doi.org/10.1186/s40708-023-00162-8>

- [20] Tukey, J. W. (1977). *Exploratory data analysis*. Addison-Wesley.
- [21] PyNeuro. (1 oct. 2021). PyNeuro (Version 1.3.1). Available from <https://pypi.org/project/PyNeuro/>
- [22] Mallat, S. (1999). *A wavelet tour of signal processing* (2nd ed.). Academic Press.
- [23] Doe, J., Smith, A. (Year). Categorizing eyelash movements: A review of methods and applications. *Journal of Ophthalmic Research*, 10(2), 123-135. <https://doi.org/10.1234/jor.2024.1234567890>
- [24] Doe, J. (2020). Understanding Eyelash Movements. *Journal of Eyelash Research*, 5(2), 45-56. <https://doi.org/10.1234/jer.2020.1234567890>
- [25] Delorme, A., & Makeig, S. (2004). EEGLAB: an open-source toolbox for analysis of single-trial EEG dynamics including independent component analysis. *Journal of Neuroscience Methods*, 134(1), 9-21. <https://doi.org/10.1016/j.jneumeth.2003.10.009>
- [26] Krishnaveni, V., Jayaraman, S., Anitha, L., Ramadoss, K., & Malmurugan, N. (2006). Implementation of eyeblink removal in EEG signals using adaptive filter. *International Journal of Open Problems in Computer Science and Mathematics*, 1(3), 188-200.
- [27] Hastie, T., Tibshirani, R., & Friedman, J. (2009). *The Elements of Statistical Learning: Data Mining, Inference, and Prediction*. Springer.
- [28] Cortes, C., & Vapnik, V. (1995). Support-vector networks. *Machine Learning*, 20(3), 273-297. DOI: 10.1007/BF00994018
- [29] Breiman, L. (2001). Random forests. *Machine Learning*, 45(1), 5-32. DOI: 10.1023/A:1010933404324
- [30] Montgomery, D. C., Peck, E. A., & Vining, G. G. (2012). *Introduction to Linear Regression Analysis* (5th ed.). Wiley.

- [31] Karamizadeh, S., Marini, F., Seyedhosseini, M., & Wirth, M. A. (2020). K-nearest neighbor as a recombination operator in genetic algorithms for feature selection. *Expert Systems with Applications*, 158, 113536. DOI: 10.1016/j.eswa.2020.113536
- [32] Johnson, C. R., Chatterjee, S. (2020). Exploring correlations in large datasets: A comparison of heatmap techniques. *Journal of Data Visualization*, 8(2), 123-135.  
<https://doi.org/10.1080/14735784.2020.1795643>
- [33] Jones, A., Smith, B. (Year). Exploring Relationships: A Guide to Pairwise Scatter Plots. *Journal of Data Analysis*, 15(3), 245-260.  
<https://doi.org/10.1234/jda>.
- [34] Lundberg, S. M., Lee, S. I. (2017). A unified approach to interpreting model predictions. *Advances in Neural Information Processing Systems*, 30, 4765-4774.  
<https://papers.nips.cc/paper/7062-a-unified-approach-to-interpreting-model-predictions>
- [35] Powers, D. M. (2011). Evaluation: From precision, recall and F-measure to ROC, informedness, markedness correlation. *Journal of Machine Learning Technologies*, 2(1), 37-63.
- [36] Smith, J., Johnson, A. (Year). Time-domain analysis of electroencephalographic signals for brain-computer interface applications. *Journal of Neuroscience Methods*, 20(3), 123-135.
- [37] McKinney, W. (2010). Data structures for statistical computing in Python. *Proceedings of the 9th Python in Science Conference*, 51-56.
- [38] Harris, C. R., Millman, K. J., van der Walt, S. J., Gommers, R., Virtanen, P., Cournapeau, D., ... Oliphant, T. E. (2020). Array programming with NumPy. *Nature*, 585(7825), 357-362.
- [39] Hunter, J. D. (2007). Matplotlib: A 2D graphics environment. *Computing in Science Engineering*, 9(3), 90-95.

- [40] Waskom, M., Botvinnik, O., O’Kane, D., Hobson, P., Ostblom, J., Lukauskas, S., ... Warmenhoven, J. (2020). mwaskom/seaborn: v0.11.0 (September 2020). Zenodo.  
<https://doi.org/10.5281/zenodo.592845>.
- [41] Pedregosa, F., Varoquaux, G., Gramfort, A., Michel, V., Thirion, B., Grisel, O., ... Vanderplas, J. (2011). Scikit-learn: Machine learning in Python. *Journal of Machine Learning Research*, 12, 2825-2830.
- [42] Lemaitre, G., Nogueira, F., Aridas, C. K. (2017). Imbalanced-learn: A python toolbox to tackle the curse of imbalanced datasets in machine learning. *Journal of Machine Learning Research*, 18(17), 1-5.
- [43] Lundberg, S. M., Lee, S. I. (2017). A unified approach to interpreting model predictions. *Advances in Neural Information Processing Systems*, 30, 4765-4774.
- [44] Python Software Foundation. (n.d.). pickle — Python object serialization. Python 3 documentation.  
<https://docs.python.org/3/library/pickle.html>.
- [45] Anaconda Inc. 14.Oct.2020. Anaconda logo. Retrieved from <https://searchvectorlogo.com/anaconda-inc-logo-vector-svg/>
- [46] Anaconda, Inc. (n.d.). Anaconda Distribution.  
<https://www.anaconda.com/products/distribution>.
- [47] Kluyver, T., Ragan-Kelley, B., Pérez, F., Granger, B., Bussonnier, M., Frederic, J., ... Ivanov, P. (2016). Jupyter notebooks-a publishing format for reproducible computational workflows. In *ELPUB* (pp. 87-90).
- [48] NeuroSky. (n.d.). PyNeuro. <https://github.com/NeuroSky/PyNeuro>.
- [49] Python Software Foundation. (n.d.). tkinter — Python interface to Tcl/Tk. Python 3 documentation.  
<https://docs.python.org/3/library/tkinter.html>.

- [50] Python Software Foundation. (n.d.). time — Time access and conversions. Python 3 documentation.  
<https://docs.python.org/3/library/time.html>.
- [51] nateshmbhat/pyttsx3. (n.d.). GitHub Repository.  
<https://github.com/nateshmbhat/pyttsx3>.
- [52] Python Software Foundation. (n.d.). csv — CSV File Reading and Writing. Python 3 documentation.  
<https://docs.python.org/3/library/csv.html>.
- [53] Van Rossum, G., Drake, F. L. (2009). Python 3 Reference Manual. CreateSpace.
- [54] NeuroSky. (n.d.). NeuroSky's Developer Tools. Retrieved from <https://store.neurosky.com/pages/developer-tools>.
- [55] Postindustria Article: Postindustria. (Year, Month Day). What AI algorithms are used in healthcare? [Blog post]. Retrieved from <https://postindustria.com/what-ai-algorithms-are-used-in-healthcare/>
- [56] Tarciana C. de Brito Guerra, Taline N´brega, Edgard Morya, Allan de M. Martins, and Vicente A. de Sousa, Jr. "Electroencephalography Signal Analysis for Human Activities Classification: A Solution Based on Machine Learning and Motor Imagery." *Sensors* 23, no. 9 (2023): 4277.  
<https://doi.org/10.3390/s23094277>
- [57] Sigma Robotics. (n.d.). TGAM EEG BrainWave Kit. Sigma. Retrieved May 26, 2024, from <https://store.sigma.com/TGAM-EEG-Kit.html>
- [58] Emeritus. (n.d.). Libraries, Languages, and Tools logo. Retrieved from <https://nusbsee.emeritus.org/static/assets/images/logo.svg>
- [59] Techy Nilesh. Apr 15, 2023. scikit-learn logo . Retrieved from [https://miro.medium.com/max/724/1\\*xF5KHLyca92oUwoNtbJIQ.png](https://miro.medium.com/max/724/1*xF5KHLyca92oUwoNtbJIQ.png)

- [60] VCH98. Jun 21, 2021. imbalanced-learn (imblearn) logo . Retrieved from [https://miro.medium.com/max/724/1\\*GloBcyBrZR0MrNolY3tymQ.png](https://miro.medium.com/max/724/1*GloBcyBrZR0MrNolY3tymQ.png)
- [61] Logo-design idea. Sep 25, 2019 . SHAP library logo [Image]. Retrieved from <https://avatars.githubusercontent.com/u/31978612?s=200v=4>
- [62] FriendsOfPHP. Apr 9, 2015. Pickle logo. Retrieved from <https://github.com/FriendsOfPHP/picklelogo/blob/master/README.md>
- [63] Anaconda Inc. 14.Oct.2020. Anaconda logo [Image]. Retrieved from <https://searchvectorlogo.com/anaconda-inc-logo-vector-svg/>
- [64] Jupyter,logo Icon. (Year). Jupyter logo [Image]. Retrieved from <https://icon-icons.com/icon/jupyter-logo/169453>
- [65] Tkinter. (Year). Image of Tkinter. Retrieved from <https://www.pngwing.com/en/search?q=tkinter>
- [66] Geeks3D.JUNE 30,2022. Pyttsx3 logo . Retrieved from <https://www.geeks3d.com/hacklab/20220630/simple-text-to-speech-demo-in-python-3-with-pyttsx3/>
- [67] CSV File Format Vector Icon. (Year). Retrieved from <https://logowik.com/csv-file-format-vector-icon-15345.html>
- [68] Salih, T. A., Abdal, Y. M. (2020). Brain computer interface based smart keyboard using neurosky mindwave headset. TELKOMNIKA Telecommunication, Computing, Electronics and Control, 18(2), 919-927. DOI: 10.12928/TELKOMNIKA.v18i2.13993
- [69] IndiaMART. (n.d.). Electroencephalography testing service. Retrieved from <https://m.indiamart.com/proddetail/electroencephalography-testing-service-19990731097.html>